# Analysis and Design of Pile in expansive soil using uplift force

By


**Akshay Ahlawat**

2234728


*Thesis*
*Submitted to Flinders University*
*for the degree of*

**Master of Civil Engineering**

Flinders University
04/08/2023

# TABLE OF CONTENTS

# DECLARATION

I certify that this thesis:

1. does not incorporate without acknowledgment any material previously submitted for a degree or diploma in any university.
2. and the research within will not be submitted for any other future degree or diploma without the permission of Flinders University; and
3. to the best of my knowledge and belief, does not contain any material previously published or written by another person except where due reference is made in the text.

Signature of student...... .............................................

Print name of student…. Akshay. Ahlawat...........................................

Date....4/08/2023..................................................

I certify that I have read this thesis. In my opinion it is/is not (please circle) fully adequate, in scope and in quality, as a thesis for the degree of Master of Civil Engineering. Furthermore, I confirm that I have provided feedback on this thesis and the student has implemented it minimally/partially/fully (please circle).

Signature of Principal Supervisor...................... ............................

Print name of Principal Supervisor.............Hongyu Qin.....................................

Date...........4/8/2023............................................

# ACKNOWLEDGEMENTS

First and finest, I would like to gratefully express my deepest acknowledgment to my academic research Supervisor, Dr. Hongyu Qin. He always displayed valuable advice to me about my progress even at the start of my thesis. He always assisted me to find research books both on academic topics and thesis. He helped me with other topics when required and helped me to learn time management to quite a degree.

He is optimistic for me as he could identify me when I was worried about some topic in class and meetings while giving hints to push me to find results on my own. His guidance on this topic will always keep a space in my career and heart.

I would like to display my appreciation to Dr. Thomas Vincent as course coordinator. His guidance on even insignificant things helped a long way to make studying easy for me.

I would like to thank Professor Branko Stazic, his enthusiasm to help on learning a topic fully is admirable.

I would like to thank Professor Rocco Zito for his fine nature, Dr. Nicholas Holyoak for his keen nature of understanding fine details, Dr. Aliakbar Gholampour being a humble nature person with accuracy on topics, Professor Adrian Werner who unlocked my potential to enjoy learning at all times, Dr. Cristina Solórzano-Rivas for amazing teaching, Professor Frank M. Wasko for his helping me to understand project financial and Jacqui from Wil who helped me in times of searching for internship.

A special thank you to Julie Zanker. Student Administration Support Assistant. Her support is special for me.

I also acknowledge my friends Chatushikha, Mohit, and Jaineel who supported me when I was low.


# LIST OF FIGURES

## LIST OF TABLES

## Abstract

In this research, a new equation was also derived using Rayleigh's method of dimensional analysis. This new equation uses the "soil suction" as key parameter to obtain pile movement in the soil. Soil suction values used for analysis chosen for different sites were based on comparing with a table where the study was performed by Snethen on Atterberg Limits (1977).

In this thesis, four sites were chosen to have expansive clay soil nature with different clay minerals type and their comparison is made in the analysis part of the thesis on net movement. Free-state province of the South Africa (between Kroonstad and Vredefort), Nanning, Guangxi Province of China, Colorado State University, Fort Collins, Colorado, and Shri Vishnu Educational Society of Andhra Pradesh, India.

An efficient pile design comparison was done on length for the design guide section of the thesis. The Rigid pier method was used for estimating length of pile required for 2 sites Free-state province and Colorado State University as pile length is not provided. Thereafter a comparison is performed for different pile bottom design types by Elastic design method, namely elastic straight shaft pier, belled pier, and helical pier (Nelson 2007). The results are presented for future design reference.

Keywords: Expansive soil, RSPile, Case Study, New method, Design Curve, Elastic Solution

# 1. EXECUTIVE SUMMARY

Dear Examiner,

I present this thesis with respect and admiration titled "Analysis and Design of Piles in Expansive Soil by uplift force only." This executive summary culminates the research objectives, various analyses in expansive clay with key findings of the research on the uplift force, and a new set of methodology guidelines for the design of piles.

The thesis has endeavoured and guided me to understand various complexity of the analysis and design of piles, with distinct attention needed on underlying principles on the expansive nature of the soil, and to resolve issues being met by the Geotech engineering community on design.

Expansive soils are types of soil that undergo swelling/heaving (or shrinkage) due to changes in moisture content. When water is ingressed by soil, volumetric change in the form of expansion (swelling) forces soils to push the pile upwards (hard bedrock beneath does not allow downward movement). The movement in this research is calculated by using a new equation which in turn is compared with other empirical equations Design curves of Poulos (1989), Elastic solution by Silva (2021), and RS pile (RocScience Software).

In this research, a new equation was also derived using Rayleigh's method of dimensional analysis. This new equation uses the "soil suction" as key parameter to obtain pile movement in the soil. Soil suction values used for analysis chosen for different sites were based on comparing with a table where the study was performed by Snethen on Atterberg Limits (1977).

In this thesis, four sites were chosen to have expansive clay soil nature with different clay minerals type and their comparison is made in the analysis part of the thesis on net movement. Free-state province of the South Africa (between Kroonstad and Vredefort), Nanning, Guangxi Province of China, Colorado State University, Fort Collins, Colorado, and Shri Vishnu Educational Society of Andhra Pradesh, India.

An efficient pile design comparison was done on length for the design guide section of the thesis. The Rigid pier method was used for estimating length of pile required for 2 sites Free-state province and Colorado State University as pile length is not provided. Thereafter a comparison is performed for different pile bottom design types by Elastic design method, namely elastic straight shaft pier, belled pier, and helical pier (Nelson 2007). The results are presented for future design reference.

# 2. INTRODUCTION

## 2.1. Background

### 2.1.1 Definitions of expansive soil with adverse effects

Expansive soil or Reactive soil is a term for soils that undergo large change in volume (shrinking and vice versa swelling) because of moisture content change in soil. These predominantly contain Hydrophilic clay minerals. (Al-Rawas et al, 1998).

Hydrophilic clay minerals have a high affinity (water-love) for adsorbing and exchanging water molecules which readily absorb and retain water inside their structure. Montmorillonite, kaolinite, and Illite are common hydrophilic clay minerals, found in all sites mentioned in this thesis.

Expansive soils have caused severe financial consequences in every continent of the world. Jones and Holtz (1973) have reported in the USA, the yearly damage to infrastructure has constituted twice as many earthquakes, hurricanes, and tornadoes combined. Correspondingly, Jones and Jefferson (2012) have pointed out that swelling clays as being the most catastrophic calamity in Britain, putting GBP 400 million per year costing towards the insurance industry.

These clays are widely encountered in the arid and semi-arid regions in the Sudan (Particularly South Sudan), Australia, India, and Tanzania (Morin, 1971) Texas, the USA, and South Africa are known to have concerns with expansive clay (Jones and Holtz 1973; Williams et al 1985).

Figure removed due to copyright restriction.

*Figure 1 Global distribution of expansive soil sites reported. (Sawangsuriya et al. 2011)*

Figure 1 shows the expansive soil sites which are distributed globally and had been reported. Taken from Sawangsuriya et al. 2011.

### 2.1.2 Expansive soil Ground Improvement

Variety of techniques are used for mitigating shrink-swell behaviour in expansive soil.

1. Excavating, removing expansive soil layer, and infilling with non-expansive soil from close by site. Is preferred when the area is not large, and the cost is not too high.
2. Using additives like cement, lime, fly ash, polypropylene fibre, and industrial wastes (Fattah et al., 2010).
3. Using pile or pier system: Pile is a deep foundation type that takes a load to weak expansive soil layers and is embedded/placed on a hard stratum layer. These can be steel, concrete, or timber types. This foundation can be end-bearing, friction, compaction, or anchor piles. Pier is also a deep foundation that is engaged deeper into the hard stratum which are normally concrete, steel, or drilled caissons.

During the wet periods of the year, increase in water content, and heaving/swelling of soil/clay causes an axial/uplift force generation into the pile (down-drag force where soil shrinkage appears in the dry season leading to settlement) (Chengfu et al, 2020).

Figure removed due to copyright restriction.

*Figure 2 Distribution of Shaft Friction, which is experienced along a pile length, before and after infiltration of moisture, Taken from Yunlong et al (2015)*

Figure 2 depicts the distribution of Shaft Friction, which is experienced along a pile length, before and after infiltration of moisture.

From the figure 2, positive shaft friction also called skin friction or side friction is resistance developed along the lateral surface of a pile as it is driven or inserted into the ground. Negative friction or down drag or negative skin friction refers to the downward force exerted on a pile due to the movement of the surrounding soil. Prior to infiltration, in unsaturated expansive soil positive side friction is dispersed along the entire length and carries load with addition from tip or end. Water infiltrates/absorbed into the soil and subsequent swelling takes place. Positive skin friction strengthens in active zone and emerges in stable zone (depth of soil where water infiltration does not influence). These swell forces pile to move up on infiltration. Net contribution from negative skin friction, tip or end bearing capacity and surcharge unite to stop from being pulled up in expansive soil; however, load-carrying capacity decreases when upward movement in the pile takes place (Yunlong et al, 2015).

The thesis will study to analyze pile movement in expansive soil using a comparative approach. This research will also help to understand different parameters related to situations of heave and how the length of the pile is affected by different shapes of pile type bottom.

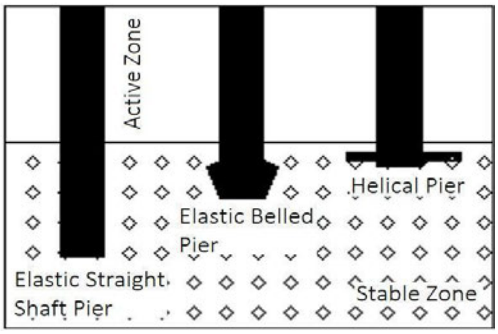


*Figure 3 Different types of pile design by bottom shapes*

Figure 3 depicts distinct types of pile design by bottom shapes.

A new equation is put into analysis where it is compared with the established Design curves by Poulos (1989), Elastic solution by Silva (2021) for theoretical analysis, total solution, and Numerical Modelling were performed using RS pile software. The new equation requires soil suction as a parameter to obtain soil movement and is derived in Literature Review. Using soil movement, axial force induced is found, and later skin friction can be derived for the chosen location scenario in the results section of the research.

Projects of these levels are important to many personnel working in the Energy Geotech field as this report will help future Geotechnical Engineers to understand the concept of uplift forces (axial force) action in expansive clay. The study investigates interaction of pile-soil and expansive soil design. This research will predict a novel approach and find its viability in comparison to other prediction methods which work to analyse piles in expansive clay and check on the design of piles by different pile type bottoms.

1. Elastic Straight Shaft Pier
2. Elastic Belled Pier
3. Helical Pier

**2.2. Scope of Thesis**

Due to time limitations on research. The study investigates interaction of pile-soil under axial loading.

Laterally loaded piles are not considered for the project scope.

The length of the pile foundation by different bottom design types is taken as the research scope.

### 2.3. Research Importance

In the Analysis part, using the method of Section 1 (Design Curves) overestimates results and thereby makes it hard for estimating soil movement, Section 2 (Elastic Solutions) is complex for application.

In the design part, Helical piers due to their design shape give the best results having small length requirements as compared to elastic and bell-shaped bottom piles.

The study helps to develop a simple guide by theory combination in section 1 and section 2 in conjunction with using new equations to reach a desired model. The advantages of models are.

1. The present model is easy to apply.
2. Require the least amount of data.
3. Offers an alternative approach to get a prediction for aspects of pile-soil interaction: vertical pile movement results for axial loads, skin friction of pile.
4. Comparison between distinct types of piers by bottom design and their application as pile.

### 2.4. Research Aims

The study focusses to provide a simplified model for the prediction of vertical pile movement with accuracy using a novel approach and comparison with complicated models using design curves and elastic solutions.

This model is established for overcoming drawbacks of different equations for separate locations.

### 2.5. The Structure of Thesis

- Part 3 - Literature Review: The part deals with an overview of the pile-soil interaction of expansive soils. Key sections are produced for verified studies.
- Part 4 - Methodology: This part explains the process of analysis and design approach for the model using theories and derivation of equations used in the model.
- Part 5 - Results and Discussion: Outcomes are presented here. Results are compared with preceding studies and RSPile results. A discussion of obtained results is provided here.
- Part 6 - Conclusions and Future Work: The outcomes are summarized and suggestions for proposed future work studies are based on the limit of the presented model.
- Appendix has RSPile software results and comparison models of analysis with the design of the pile.

# 3. Literature Review

This Literature review provides an analysis overview and design considerations on piles in expansive clay soil. Expansive clay soil exhibits significant problems due to clay soil volume change and other associated issues.

## 3.1. Expansive Soil Terminologies

### 3.1.1. Adhesion Factor

Adhesion is the tendency of dissimilar particles (or surfaces) to be attracted to one another.

The adhesion factor, α, is a coefficient that computes the bond strength or adhesion between the surface of the pile and the surrounding soil. It depicts the ratio of adhesion force to effective vertical stress working in between pile-soil interfaces.

The adhesion factor decreases slightly for dry or optimum samples with moisture while it increases linearly with moisture for moisture content higher than the plastic limit. An adhesion factor of 0.45 may be adopted for moisture content lower than the plastic limit (PL) of the soil. Elsharief (1987) had conducted out direct shear apparatus in the similar adhesion tests in the Sudanese clays and the results of the tests were used for obtaining adhesion factor equation (moisture content, $m_c$ in percentage) above the plastic limit.

$$\alpha = 0.045\, m_c - 0.407 \tag{1}$$

### 3.1.2. Depth of Wetting

Depth of Wetting, also known as wetting front depth, is the vertical distance where saturation or water infiltration takes place in soil contour depth. It is a depth where due to the presence of water moisture content in soil increases significantly. After Irrigation or rainfall, water infiltration into the soil surface and downward moves gradually, increasing moisture content with depth.

Zone of Seasonal Moisture Fluctuation is a soil zone, were due to rainfall climatic change and evapotranspiration, water content changes in a year. It is a depth where moisture content in soil undergoes momentous variation between dry and wet periods of the year.

The active depth of soil, also known as the Active zone or the active soil layer, refers to soil profile depth where seasonal volumetric changes due to soil moisture content variations. Active Depth ($H_s$) is the depth where volumetric change happens in soil suction due to climate changes at the ground surface (Fityus & Delaney 2001). An active Zone is a zone where heave contributes to soil expansion at a particular point in time. The change of depth of the active zone takes place due to heave progression and varies with time.

Designing the active zone of soil, also called design depth of expansive soil or design depth of active zone is depth calculation at which volume changes are expected to occur due to fluctuations in moisture in expansive soil. The depth which contributes to heaving where the foundation structure is designed is the design active zone ($Z_{ad}$).

Depth of Potential Heave, also known as heave zone or heave-prone zone is defined as the depth of soil profile where heaving or upward movement by expansive soil swelling by water induction. It is also depth where the swelling pressure of soil is equaled or exceeded to overburden vertical stress. The calculation of the maximum depth occurring for the Active zone is beneficial to engineers to reduce heave effects.

### 3.1.3. Ground Surface Movement (Heave)

Soil Movement (or heaving) occurs wherein water enters within clay minerals and causes an increase in the volume of soil and subsequent lifting up of structure in an upward direction.

The soil depth which contributes to heave at any instance of time depends usually upon many parameters. However, for the prediction of heave, these factors need to be considered.

1. Soil Type and profile composition - the soil type affects the magnitude of soil movement. Where Expansive soils (clay soils) absorb water and swell during wet seasons.
2. Depth and degree of wetting of soil
3. Initial and final effective stress state condition with cohesion/adhesion details
4. Groundwater conditions

Free-field heave is a type of movement that takes place due to no other load applied to soil such as by a foundation or a structural embankment. Heave varies proportionally linear along the depth, starting with maximum value (So) at the Ground level surface to being zero at active depth (Zhang et al. 2007, Poulos and Davis 1980).

Pier heave rate depends on the proportion to which sub-soil becomes wetted. Analysis of the rate of wetting of soil movement is done for cases where a constant source of water at the ground surface, have shown that water movement toward subsoil for up to ten meters can require in between 20 to 30 years or sometimes more (Durkee, 2000).

### 3.1.4. Soil Suction

Soil suction, also called matric suction or pore water suction can be defined as the negative pressure or tension due to capillary force within the soil matrix. It depicts the ability of soil to retain water against gravitational force.

Soil suction is created from forces of attraction between molecules of water and solid particles within soil space. A meniscus is generated in the capillary space of soil by these forces which generate suction. The magnitude of soil suction is impacted by factors such as pore size distribution, soil texture, organic matter, and water content.

Total soil suction, also called total suction or total stress suction, comprises two components in the soil system: metric suction and osmotic suction. It is the sum of both capillary forces due to water retention and osmotic forces which result from the existence of dissolved solutes in pore water.

The matric suction occurs between soil particles and water molecules due to forces of attraction. It is responsible for retaining water against gravitational force and is the dominant part of soil suction. Matric suction varies on factors such as particle size distribution, pore structure, and soil texture.

Water is also attracted to soil because of dissolved salt concentration in soil water. Salt cations have a high affinity for water and when the concentration exceeds in comparison to other external sources, water is attracted/pulled towards the soil. However due to restriction occurring in-between soil particles when space is filled. Water is pulled into tension due to the attractive nature of soil cation; this soil suction is termed osmotic suction.

## 3.2. Elementary methods of analysis of expansive soil

Many methods exist for the estimation of uplift force generated on a pile by heaving in soil. Please see Appendix A for Design Steps for each method.

### 3.2.1. Design Curve Method

Poulos and Davis (1980) introduced using Design Curves for analysis wherein applying specified movement of soil (induced by soil heave) for calculating tension in a pile. This was based on a load transfer method to make an elastic analysis method based on using curves.

### 3.2.2. Elastic Solution

Xiao et al. (2011) and Fan et al. (2007) introduced a method that uses the movement of soil against a pile to find the axial force ($P_u$) as a function of depth (z). Upward movement induced in soil or pile and tension in the pile is negative in this method. Herein movement of soil against the pile is defined using shear deformation of soil where results were validated against lab model testing (Fan et al., 2007) and a similar result was performed by Poulos and Davis (1980). Jiang et al. (2020) considered a linear variation of depth with a shear modulus of soil ($G_s$) (constant moduli used by Fan et al. (2007) and Xiao et al. (2011)).

Constants was later refined by Silva et al. (2022) for using equations he had included method from Jennings (1962) and Van der Merwe (1964) for prediction of soil heaving at the soil surface.

Table 1 depicts improvements made to Elastic solution constants to get better results by different researchers. Firstly, Fan (2007) introduced constants which were improved by Xiao (2011) and at last refined by Silva (2022)

*Table 1 shows improvements made to Elastic solution constants by different authors.*

| | Fan et al. (2007) | Xiao et al. (2011) | Silva et al. (2022) |
|---|---|---|---|
| C3 | $\frac{-S_o}{\alpha\, h_o}$ | $\frac{-S_o}{\alpha\, h_o}$ | $\frac{-S_o}{\alpha\, h_o}$ |
| C4 | $C6 - \frac{s_o \sinh(\alpha\, h_o)}{\alpha\, h_o}$ | $\frac{C6 - s_o \sinh(\alpha\, h_o)}{\alpha\, h_o}$ | $C6 + \frac{s_o \sinh(\alpha\, h_o)}{\alpha\, h_o}$ |
| C5 | $C3 + \frac{s_o \cosh(\alpha\, h_o)}{\alpha\, h_o}$ | $\frac{C3 + s_o \cosh(\alpha\, h_o)}{\alpha\, h_o}$ | $C3 + \frac{s_o \cosh(\alpha\, h_o)}{\alpha\, h_o}$ |
| C6 | $\frac{- s_o \cosh(\alpha L)(\cosh(\alpha\, h_o) - 1)}{\alpha\, h_o \sinh(\alpha L)}$ | $\frac{- s_o \cosh(\alpha L)(\cosh(\alpha\, h_o) - 1)}{\alpha\, h_o \sinh(\alpha L)}$ | $\frac{-\cosh(\alpha L)}{\sinh(\alpha L)} C5 = \frac{- s_o \cosh(\alpha L)(\cosh(\alpha\, h_o) - 1)}{\alpha\, h_o \sinh(\alpha L)}$ |

## 3.3. Dimensional Homogeneity

When dimensions (powers of fundamental dimensions i.e., L, M, T) of each term on either side of the equation are the same; the equation is known as a dimensionally homogeneous equation.

If the number of variables involved in a physical phenomenon is known, the relation among the variables can be determined by mentioned below two methods.

1. Rayleigh's Method
2. Buckingham $\pi$ Theorem

**Rayleigh's Method**

This method is useful when only three or four variables are expressed in an equation.

Let X is a variable, which depends on variables $X_1, X_2,$ and $X_3$. X is a function of $X_1, X_2,$ and $X_3$ and written as X = f $[X_1, X_2, X_3]$ or X = $KX_1{}^a, X_2{}^b, X_3{}^c$. Here K is a constant. The values of arbitrary powers a, b, and c are obtained by comparing fundamental dimension powers on both sides. Considerations for choosing variables are given as

1. Repeating variables selected should not form dimensionless group.

2. Repeating variables together must have same number of fundamental dimensions.

3. No two repeating variables should have same dimension.

## 3.4. Pile Foundation Design

Rigid pile is a type of deep foundation element providing load-bearing support for structures.

An elastic pile, also called a flexible pile, is a type of deep foundation element that shows more flexibility or deformation under loading. These piles undergo deflection and distribute load through their elastic deformation.

The anchorage force of a pile, also called pile uplift capacity or pile anchorage capacity, defines resistance against tension loads or uplift forces provided by piles. It is the ability of a pile to transfer tensile loads effectively from structure to underlying soil.

#### 3.4.1. Rigid Pier Method

- In this method, the uplift axial force is equated to anchorage force assuming a pier has no heave.
- The critical pile length design is based on axial stress equilibrium only where pile size design is predicated on minimizing the pile head movement for the pile performance.
- The skin friction is Coulomb skin friction in uplift and anchorage zones. The friction force is equivalent to net normal stress acting on the side of the pier times the coefficient of friction (Chen 1988; Nelson and Miller 1992).

#### 3.4.2. Elastic Pier Method

- In this method, uplift skin friction is considered uniform along the length of the pier or increases with depth.
- When the soil has the same swelling pressure throughout, the distribution is uniform throughout. This is a uniform distribution case.
- Cases for linear increasing distribution occurs where several strata of soils exist with deeper soils having a higher expansion potential (Nelson and Miller 1992).
- Method uses design curves.
    1. Normal pier heave plotted as a function of pier length to potential depth for heave.
    2. Normalized maximum tensile force plotted as a function of pier length to potential depth for heave.

#### 3.4.3. Pile Types by Bottom shapes

***Elastic Straight shaft pier***

Straight shaft piers are piers with side wall friction and end bearing carrying assigned design loads.

***Elastic Belled pier***

Belled or under-reamed piers are piers with a bottom bell-shaped or an under ream. A high percentage of imposed load on the pier top is carried by the base.

***Helical pier***

The principle of design is that the pull-out capacity of helical bearing plates plus dead load must resist the total uplift force exerted on the pier. The swelling pressures which act on the pier above the design active zone and other parts of the foundation system produce uplift forces. (Nelson et al, 2015)

Figure removed due to copyright restriction.

*Figure 4 Different pier types by bottom design (Nelsons 2015)*

Figure 4 shows different pier types by bottom shapes with loading mechanism

## 3.5. RSPile Software

RSPile is a program developed by Rocscience. RSPile is widely used for the analysis of pile-soil interaction under uniaxial or lateral loading or both. In this report, RSPile results generated from modelling were used for validation.

Figure removed due to copyright restriction.

*Figure 5 (a) Load transfer mechanism in piles axially loaded and (b) spring mass model. Taken from Rocscience (2022)*

RSPile uses finite element analysis by estimation of t-z curve. The stress-strain relation in case of pile loaded axially is described through 3 loading mechanisms: Pile axial deformation, soil skin friction on shaft, and soil end bearing (Figure 5 a). Using a spring-mass model to represent material stiffness by springs, numerical techniques are employed to conduct load-settlement analysis (Figure 5 b).

Using Spring-mass model, a non-linear stiffness curve is prepared by RSPile based on Finite element analysis to show stress-strain behaviour of soil. Hence, RSPile is able to provide high accurate interpretations of pile-soil interaction in expansive soil for axial loading, and settlement of pile head.

Calculation in RSPile is based on methodology by Loehr and Brown (2008).

Figure removed due to copyright restriction.

*Figure 6 shows force equilibrium in pile segment based on methodology by Loehr and Brown (2008)*

The force equilibrium equation at each calculation node $i$ is as follows.

$$(Q_z)_{i+1} = (Q_z) + (f_s)_i \qquad (2)$$

where $z$ = depth to midpoint of pile segment

$(Q_z)_{i+1}$ = top axial force of pile segment at calculation node $i+1$

$(Q_z)$ = bottom axial force of pile segment at calculation node $i$

$(f_s)_i$= soil skin friction at depth $z$ for calculation node $i$

The software runs an iterative process for solving the internal force of the pile. Solution of the toe settlement and calculation of end bearing resistance from load transfer curve due to assumed settlement. Soil skin friction is obtained by assuming a displacement in the soil at the midpoint of the pile segment, getting the load corresponding from the load transfer curve, and verifying the assumed displacement of soil from force equilibrium considering pile axial tension or compression due to assumed displacement. The equation above is used for calculating force equilibrium at each node from toe to head as the computation progresses.

# 4. METHODOLOGY

This part of the research explains the development of a guideline with a demonstration of its validation. A new equation is developed in this study which is used for analysis of vertically loaded piles in expansive clay. A new method is prepared using different equations from researchers, this method can serve as guideline which is validated using numerical analysis performed for comparison.

## 4.1. Pile-Soil interaction

Figure 5B shows an increase in positive friction prior to water infiltration along the entire length of the pile to carry pile head load plus pile end resistance. However, as water percolates into the active zone, suction reduction and suction-induced volume expansion of expansive soil significantly influence the load transfer and movement of the pile. In this scenario, mobilized lateral swelling pressure is increased additionally to lateral earth pressure as shown in Figure 5A. With the decrease in soil suction, there is a reduction in pile-soil shear strength at the interface. The relative pile-soil shear displacement uplifts the pile due to ground heave. Negative friction arises in active zone depth when the pile is uplifted in the active zone due to an increase in positive friction.

Figure removed due to copyright restriction.

*Figure 7 shows load transfer mechanism variations in unsaturated soils in piles. There is a notable change in volume shown upon infiltration which is obtained from Liu et al (2021)*

Collapsible soil behaviour is shown in Figure 5C for a typical pile. Like expansive soil behaviour, properties of the interface shear strength decrease with a reduction in suction associated with water infiltration. Soil collapse contributes to ground settlement which relates to the downward movement of soil relative to the pile. Negative friction is generated in the active zone due to this reason. Which in turn, both the pile base pressure and stable zone having positive friction increase to balance the additional load contribution from negative friction. The shaft friction is influenced by four key factors including net normal stress (lateral earth pressure), suction, interface shear strength properties, and pile-soil relative displacement. (Liu et al 2021).

The influence of vertical loads, pile diameter, longitudinal steel ratio, length of pile, and type of soil affects the response of piles in soil (Houda et al 2017).

## 4.2. New equation developed to be used in Analysis of Vertically Loaded Piles in Expansive Soil

1. **Conclusions from section 3.1, needed for derivation of simple relationship between pile displacements.**

   1.1. The pile-soil interaction is influenced by four key factors including net normal stress (lateral earth pressure), **suction**, interface shear strength properties, and pile-soil relative displacement. (Liu et al 2021).
   1.2. **The influence of vertical loads**, **pile diameter**, longitudinal steel ratio, **length of pile**, and type of soil affects the response of piles in soil (Houda et al 2017).
   1.3. Finite element analysis in RSPile is based on pile stiffness approach where using a spring-mass model to represent material stiffness by springs, numerical techniques are employed to conduct load-settlement analysis. (Rocscience (2022).

2. **Derivation of an equation**

   In this study, I proposed a new equation for the calculation of pile movement by soil action without external loading application.

   Using Rayleigh's Method of dimensional analysis herein, we can derive an equation using parameters that influence Pile movement from different conclusions as obtained from section 4.2 part 1. Pile movement ($w_p$) depends upon these parameters are listed in Table 2.

*Table 2 Parameters for pile movement derivation*

| | **Parameters** | **Dimensional Unit** |
|---|---|---|
| **1** | Soil Suction ($S_u$), kPa | $M\,L^{-1}\,T^{-2}$ |
| **2** | Perimeter of Pile (P), meters | $L$ |
| **3** | Length of Pile (L), meters | $L$ |
| **4** | Stiffness of Pile (K), kN/m | $M\,T^{-2}$ |

Pile Movement/uplift (meter) $w_p = \frac{S_u P L}{K}$ (3)

The derivation of this equation is shown in appendix A.

3. Soil Suction calculation parameter

For necessary parameters to be used for the equation, Soil suction (S) is needed which can be derived from table 3 using Atterberg Limits (Snethen et al 1977).

However, other studies have been performed in past by different researchers like Nayak and Christensen on Plasticity Index, & Percent Clay (1971), and Yoder & Witczak on percent swell (1975).

*Table 3 Relation between Liquid Limit, Plasticity Index, Soil suction, and Potential volume change (Snethen et al 1977)*

Figure removed due to copyright restriction.

## 4.3. New method developed for Analysis of Vertically Loaded Piles in Expansive Soil

1. Calculation of soil mineral type

Atterberg limits and clay content can be combined into a parameter called Activity, $A_c$. Skempton (1953) termed it. Table 4 depicts relation between Activity of clay and clay minerals (Skempton 1953) and can be predicted using plasticity index values.

Activity $(\ )_c = \frac{Plasticty\ Index}{\%\ by\ weight\ finer\ than\ 2\mu m}$ (4)

*Table 4 Typical Activity values for Clay minerals (Skempton 1953)*

Figure removed due to copyright restriction.

Table 7 shows relation between Plasticity Index, Moisture content, Free-swell value, and swell potential class.

2. Design length required

Design length was found out using rigid method of Nelson and Miller (1992). The design steps are explained in appendix B. Some necessary parameters needed for design of length is derived in sections 2.1 & 2.2. Detailed design solutions are given in Appendix C.

2.1. Expansion potential nature and Free-Swell Value

Table 5 shows relation between Expansion potential and free-swell value of soils with plasticity index, and Classification standard for expansive soils (CMC 2004).

*Table 5 Classification Standard for expansive soils (CMC 2004)*

Figure removed due to copyright restriction.

2.2. Swelling pressure is calculated using Vijayvegiva and Ghazzaly (1973)

$$Log\, P_s\, (\frac{tons^2}{ft}) = 1/19.5 \times (\gamma_d + 0.65LL - 139.5) \quad (5)$$

$\gamma_d$ = dry density (kN/m3)

$LL$ = Liquid Limit

3. Stiffness of pile (K)

Stiffness is resistance of an elastic body to deflection or deformation by applied force.

$$K = \frac{P}{\delta} \quad (6)$$

P = Axial Applied Force (kN)

$\delta =$ deflection (m)

We know that $\delta = \frac{F\,L}{A\,E}$ , (7)

So, solving (6) & (7) equation, we get

$$K = \frac{AE}{L} \quad (8)$$

$A$ = Area of top of Pile ($m^2$)

$E$ = Modulus of Elasticity of pile material (kPa)

$L$ = Length of Pile (m)

4. Axial Force (or Uplift Force)

Using Pile movement derived above, we can calculate net movement, which is sum of axial force loading and swelling (equation from Design Curve of Poulos, 1987)

$$\rho = \frac{\mathrm{P}\, I}{E_s\, D} \quad (9)$$

where, $\mathrm{P}$ = axial load applied (kN)

$\rho$ = axial movement (m) or settlement

$E_s$ = modulus of elasticity of soil (MPa)

D = diameter of pile (m)

L = length of pile

$$I = I_o\, R_k\, R_b\, R_v \quad (10)$$

$I_o$ = settlement-influence factor for incompressible pile in semi-infinite mass, for Poisson's ratio $v_s$ = 0.5

$R_k$ = correction factor for pile compressibility

$R_b$ = correction factor for bearing stratum stiffness

$R_v$ = correction factor for settlement

The correction factor's $I_o, R_k, R_b, and\ R_v$ is solved from Appendix A. Poulo's design section.

Net movement = $\rho - w_p$ (11)

5. Total Uplift force

$$P_u = \alpha\, c_u\, \pi\, D\, Z_a \quad (12)$$

$c_u$ = Undrained shear strength of soil

$Z_a$ = Active layer depth

$\alpha$ = pile shaft adhesion factor (0.45 is recommended by Elsharief et al. 2016; Byrne et al 2019).

6. After the calculation of Uplift force, we can use the Skin Friction formula for calculation.

$$F = \frac{Pu}{A} \tag{13}$$

F = skin friction (kPa)

A = surface area of pile = $\pi$ * D * L ($m^2$)

## 4.4. RSPile Software Analysis Steps

1. Home Tab > Project Settings. In Pile Analysis Type > Individual Pile analysis > Axially loaded piles.
2. Soils Tab > Define soil properties. Add in soil/clay properties – Unit weight, type, shear strength, max unit friction permissible and end bearing resistance.
3. Soils Tab > Edit all boreholes. Insert Layers and define by thickness.
4. Piles Tab > Pile sections. Define pile section properties dialog. Adding section type, cross section, diameter & thickness size, and Young's modulus.
5. Piles Tab > Single. Add pile and choosing geometry to add Length and pile elevation needed. Choose Loading tab to add dead load.
6. In displacement tab under "add piles", we consider ground movement. Here we can replicate heaving/vertical movement by adding vertical displacement values.
7. Placement of Piles and generating results.

## 4.5. Comparison of different Pier bottom design types

A comparison study is also performed on different pier bottom design types on basis of length. The study is performed after prediction of free-field heave by Nelson and Miller (1992) is done using Rigid Pier method. Elastic method curves for designing pile by different bottom shapes are shown with steps in Appendix B in conjunction with Rigid pier method for required length.

# 5. RESULTS

Here data from four case sites that were studied by previous researchers are individually presented for analysis and their comparison against different methods are shown in figures & tables. Design of pile length required for 2 cases are done Colorado State university (Case Study 1) and Free-state province (Case Study 2) with solutions entailed in Appendix C. The Comparison values needed for design of pile length on basis of different pile by bottom shape types are also summarized in Appendix C.

Detailed analytical results for Poulos Design Curve and this study are summarized in Appendix D. Silva's result using excel program are summarized in Appendix E. Numerical Results from RSPile are summarized in Appendix F.

## 5.1. Case Study 1. Colorado State University (USA) Test site in Pierre shale formation

The study used parameters for a study conducted by Nelsons (2007). The diameter of the borehole is 250 mm. The maximum tolerable movement of the foundation soil is 50 mm.

Figure removed due to copyright restriction.

*Figure 8 Soil profile chart from Colorado State University, Fort Collins, Colorado*

Figure 8 shows the soil profile chart from Colorado State University, Fort Collins, Colorado. Table 6 shows results from lab showing Liquid limit (LL), Plastic limit (PL), Plasticity Index (PI), Specific Gravity, Optimum moisture content (OMC), and Maximum dry density (MDD) are summarized. Table 7 shows oedometer test data from site.

*Table 6 Soil data for Colorado State University, Fort Collins, Colorado.*

| Description | Group Symbol | Total Suction (kPa) | Specific Gravity | Optimum Moisture Content (%) | Maximum Dry Density (gm/cm3) |
|---|---|---|---|---|---|
| Pierre Shale formation | CH | 393 | 2.71 | 30 | 1.55 |

*Table 7 Oedometer data for Colorado State University, Fort Collins, Colorado*

| Oedometer data | | | | | Consolidation-Swell Test Inundation pressure = 48 kPa | |
|---|---|---|---|---|---|---|
| Soil Type | Height (m) | Water Content (%) | Expansive Potential | Total Density (Mg/m3) | Percent Swell (%) | Swelling Pressure (kPa) |
| Native Clay | 3 | 15.0 | 1.1 | 1.84 | 2.0 | 240 |
| Claystone | 4 | 10.0 | 2 | 1.94 | 3.0 | 335 |

**Analytical Results**

Table 8 represents analytical results for Colorado State University, Fort Collins, Colorado. Here results are shown which were obtained from Design Curve by Poulos (1991), Elastic Method using constants from Silva (2012), RSPile software, and this study.

*Table 8 Analytical Results for Colorado State University, Fort Collins, Colorado*

| | (Poulos, 1991) | (Silva, 2022) | RSPile | This study |
|---|---|---|---|---|
| Max axial force induced (kN) | 94.7 | 157.73 | 200.12 | 140.65 |
| Max skin friction (kPa) | 6.24 | 5.207 | 12.98 | 9.25 |
| Max net upward movement (mm) | 6.33 | 10.8 | 16.1 | 15.8 |

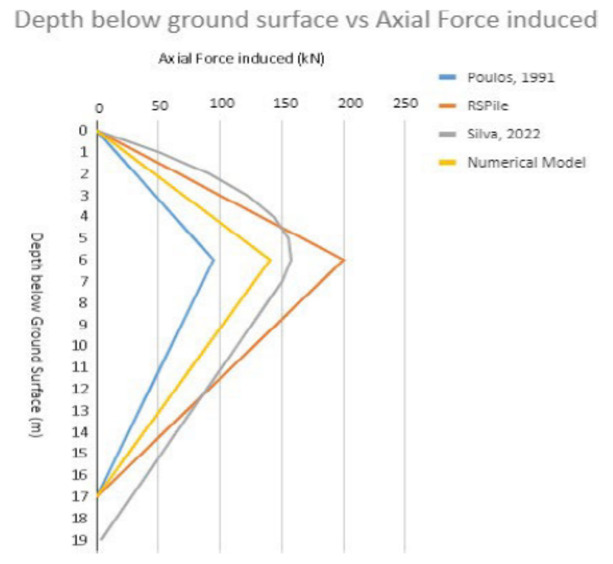


*Figure 9 Chart between Depth below ground surface (GL) vs Axial force induced (kN)*

Figure 9 demonstrates comparison between Depth below ground surface (GL) vs Axial force induced (kN). The site is Colorado State university. This study falls close in results as compared to Poulo's Design curve method (1991), Elastic Stress Method using constants of Silva (2022), and RSPile software.

All models describe there is an increase in maximum axial load induced up to active zone depth. The active depth increases from 0 to 3 m, the axial force induced also increases from 0 to 220.66 kN (RSPile), 0 to 234.21 kN (Silva, 2022), 0 to 311.2 kN (Poulos, 1991) and 0 to 289.48 kN (This study). The variation between this study with RSPile is 43 %.

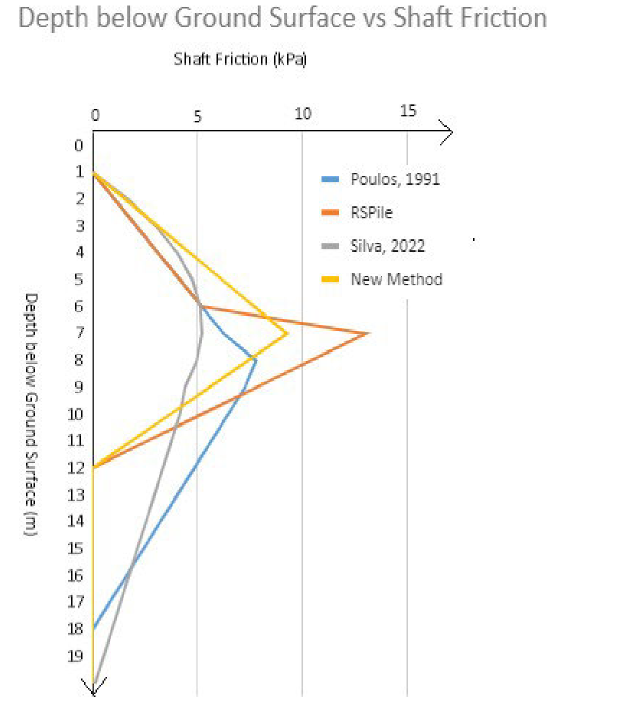


*Figure 10 Chart between Depth below ground surface (GL) vs Skin friction (kPa)*

Figure 10 demonstrates comparison between Depth below ground surface (GL) vs Skin friction (kPa). The site is Colorado State university. This study falls close in results as compared to Poulo's Design curve method (1991), Elastic Stress Method using constants of Silva (2022), and RSPile software.

All models describe there is an increase in maximum skin friction on pile-soil interface up to active zone depth. The active depth increases from 0 to 3 m, the skin friction also increases from 0 to 12.98 kPa (RSPile), 0 to 5.207 kPa (Silva, 2022), 0 to 6.24 kPa (Poulos, 1991) and 0 to 9.25 kPa (This study). The variation between this study with RSPile is 40.3 %.

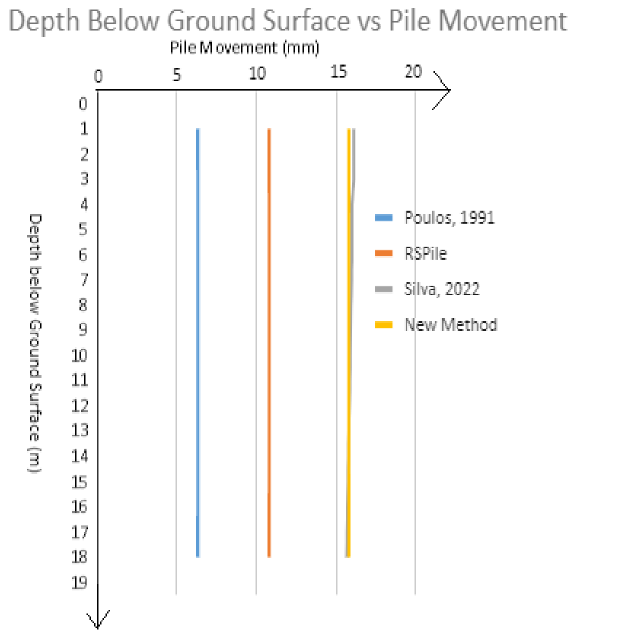


*Figure 11 Chart between Depth below ground surface (GL) vs Soil movement (mm) upward induced*

Figure 11 demonstrates comparison between Depth below ground surface (GL) vs Soil movement (mm) upward induced. The site is Colorado State university. This study falls close in results as compared to Poulo's Design curve method (1991), Elastic Stress Method using constants of Silva (2022), and RSPile software. All models describe there is an increase in maximum net movement in between soil swelling upwards and pile settlement downwards. There is an upward movement which is maximum at ground level at 4.07 mm (RSPile), 5.4 mm (Silva, 2022), 6 mm (Poulos, 1991) and 5.3 mm (This study). The variation between this study with RSPile is 2 %.

Chart Figures 9, 10, and 11 presents the results of this study, Poulo's Design Curve model, Silva's Method and RSPile's model. Figures in table 12 demonstrates present model, which is close, implicating that present model can be easily used for estimation of pile-soil interaction in Colorado expansive soil with good level of accuracy compared with those models.

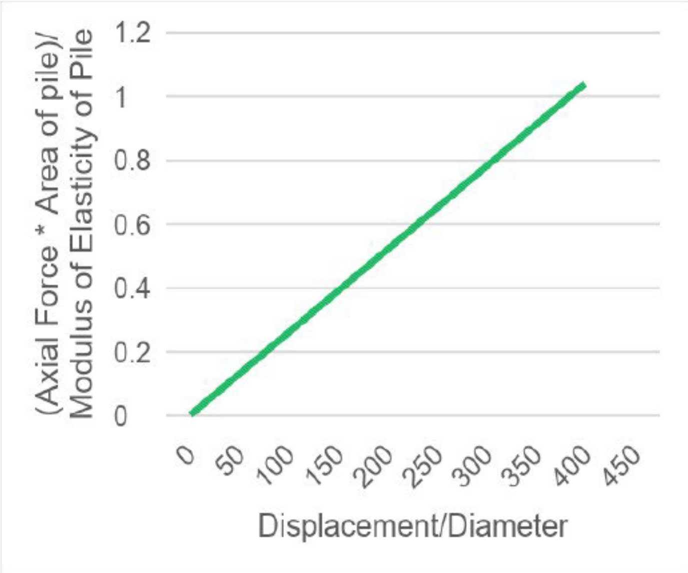


*Figure 12 shows linear relation is established for soil movement against axial force induced in Colorado, USA expansive soil site*

This chart of figure 12 is prepared where vertical axis is $\frac{Axial\ Force\ *\ Area\ of\ pile}{Modulus\ of\ Elasticity\ of\ Pile}$ is put against horizontal axis of $\frac{Displacement\ of\ pile}{Diameter\ of\ pile}$ This graph shows a linear relation is established for soil movement against axial force induced in expansive soil without any external dead load applied.

**Pile Design**

Table 9 represents the pile length design results from Colorado State University, Fort Collins, Colorado. Here the difference in between length of Rigid pier against Straight shaft pier (5.89 %), Belled pier (41.97 %) and Helical pier (68.63 %) design type.

When comparison in between Elastic belled pier and Helical pier is performed. The difference is in range of 45.95 %. A comparatively good difference in length and thus saving in cost in design phase.

*Table 9 Length required for different pile types by bottom shape in Colorado State University, Fort Collins, Colorado*

| | Rigid Pier | Elastic Straight Shaft Pier | Elastic Belled Pier | Helical Pier |
|---|---|---|---|---|
| Length of Pile Required (m) | 19.3 | 16.5 | 9.9 | 5.2 |

## 5.2. Case Study 2. Free state province of South Africa (b/w Kroonstad and Vredefort)

Burke (2022) conducted study where the site is situated in an alluvium plain underlain by lavas of Klipriviersberg group (basalt and andesite igneous rocks). Potential expansiveness of samples using plasticity index (PI) fall within the high expansive region. The borehole diameter was 450 mm. Tolerable swelling at the surface is 56 mm and active depth is 7 m.

Table 10 depicts Soil data from Lab for Free-state province of South Africa (b/w Kroonstad and Vredefort). Here results showing Liquid limit (LL), Plastic limit (PL), Plasticity Index (PI), Specific Gravity, Optimum moisture content (OMC), and Maximum dry density (MDD) are summarized. Table 11 shows oedometer test data from site.

*Table 10 Soil data from lab for Free state province of South Africa (b/w Kroonstad and Vredefort)*

| Description | Group Symbol | LL % | PL % | PI % | Specific Gravity | Optimum Moisture Content (%) | Maximum Dry Density (gm/cm3) |
|---|---|---|---|---|---|---|---|
| Dark grey sandy silty clay | CH | 65 | 22 | 43 | 2.65 | 21.07 | 1.486 |

*Table 11 Oedometer data for Free state province of South Africa (b/w Kroonstad and Vredefort)*

| Oedometer data | | | | | Consolidation-Swell Test Inundation pressure = 45 kPa | |
|---|---|---|---|---|---|---|
| Soil Type | Height (m) | Water Content (%) | Expansive Potential | Total Density (Mg/m3) | Percent Swell (%) | Swelling Pressure (kPa) |
| Native Clay | 7 | 12.8 | 1.1 | 1.76 | 8.0 | 139 |

**Analytical Result**

Table 12 represents the analytical result from Free-state province of South Africa (b/w Kroonstad and Vredefort)

*Table 12 Analytical result for Free-state province of South Africa (b/w Kroonstad and Vredefort)*

| | (Poulos, 1991) | (Silva, 2022) | RSPile | This study |
|---|---|---|---|---|
| Max axial force induced (kN) | 450 | 628.05 | 680 | 566.89 |
| Max skin friction (kPa) | 8.94 | 12.48 | 13.49 | 11.26 |
| Max net upward movement (mm) | 8.01 | 12.7 | 16.1 | 24.8 |

| | |
|---|---|
| 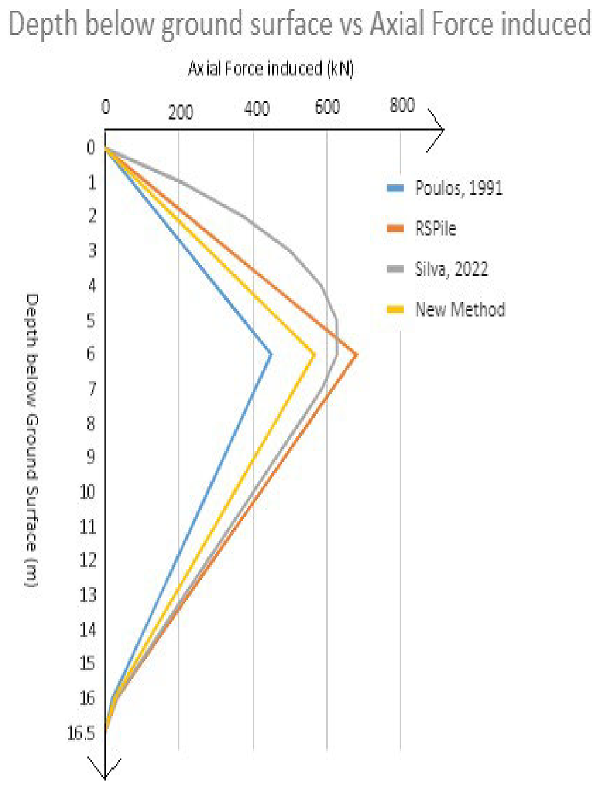<br>*Figure 13 Chart between Depth below ground surface (GL) vs Axial force induced (kN)* | Figure 13 demonstrates comparison between Depth below ground surface (GL) vs Axial force induced (kN). The site is Free-state province of South Africa (b/w Kroonstad and Vredefort). This study falls close in results as compared to Poulo's Design curve method (1991), Elastic Stress Method using constants of Silva (2022), and RSPile software.<br>All models describe there is an increase in maximum axial load induced up to active zone depth. The active depth increases from 0 to 7 m, the axial force induced also increases from 0 to 680 kN (RSPile), 0 to 628.05 kN (Silva, 2022), 0 to 450 kN (Poulos, 1991) and 0 to 566.89 kN (This study). The variation between this study with RSPile is 20 %. |
| 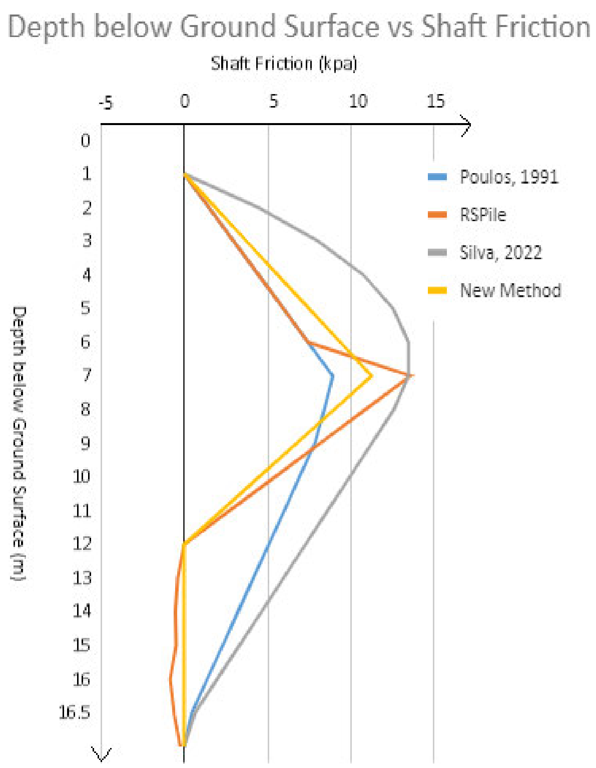<br>*Figure 14 Chart between Depth below ground surface (GL) vs Skin friction (kPa)* | Figure 14 demonstrates comparison between Depth below ground surface (GL) vs Skin friction (kPa). The site is Free-state province of South Africa (b/w Kroonstad and Vredefort). This study falls close in results as compared to Poulo's Design curve method (1991), Elastic Stress Method using constants of Silva (2022), and RSPile software.<br>All models describe there is an increase in maximum skin friction on pile-soil interface up to active zone depth. The active depth increases from 0 to 7 m, the skin friction also increases from 0 to 13.49 kPa (RSPile), 0 to 12.48 kPa (Silva, 2022), 0 to 8.94 kPa (Poulos, 1991) and 0 to 9.25 kPa (This study). The variation between this study with RSPile is 46 %. |

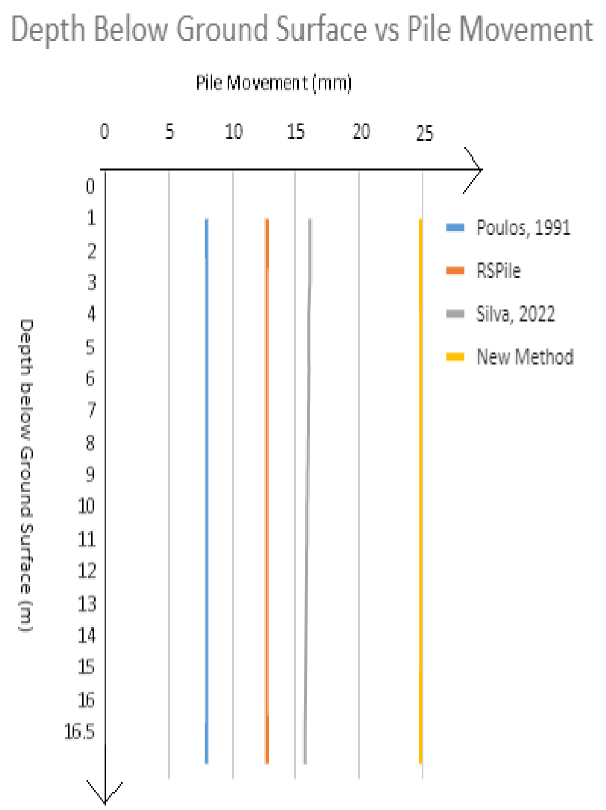


*Figure 15 Chart between Depth below ground surface (GL) vs Soil movement (mm) upward induced*

Figure 15 demonstrates comparison between Depth below ground surface (GL) vs Soil movement (mm) upward induced. The site is Free-state province of South Africa (b/w Kroonstad and Vredefort). This study falls close in results as compared to Poulo's Design curve method (1991), Elastic Stress Method using constants of Silva (2022), and RSPile software. All models describe there is an increase in maximum net movement in between soil swelling upwards and pile settlement downwards. There is an upward movement which is maximum at ground level at 16.1 mm (RSPile), 12.7 mm (Silva, 2022), 8.01 mm (Poulos, 1991) and 24.8 mm (This study). The variation between this study with RSPile is 36 %.

Figures 13, 14, and 15 presents the results of this study, Poulo's Design Curve model, Silva's Method and RSPile's model. Figure demonstrates present model, which is close, implicating that present model can be easily used for estimation of pile-soil interaction in Province expansive soil with good level of accuracy compared with those models.

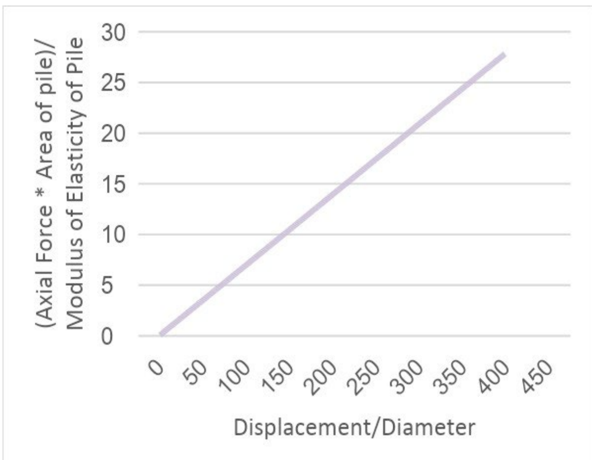


*Figure 16 shows linear relation is established for soil movement against axial force induced in Free State Province, South Africa expansive soil site.*

This chart of figure 16 is prepared where vertical axis is $\frac{Axial\ Force\ *\ Area\ of\ pile}{Modulus\ of\ Elasticity\ of\ Pile}$ is put against horizontal axis of $\frac{Displacement\ of\ pile}{Diameter\ of\ pile}$ This graph shows a linear relation is established for soil movement against axial force induced in expansive soil without any external dead load applied.

**Pile Design**

Table 13 represents the pile length design results from the Free-state province of South Africa (b/w Kroonstad and Vredefort). Here the difference in between length of Rigid pier against Straight shaft pier (14.51 %), Belled pier (48.71 %) and Helical pier (73.06 %) design type. When comparison in between Elastic belled pier and Helical pier is performed. The difference is in range of 47.48 %. A comparatively good difference in length and thus saving in cost in design phase.

*Table 13 Length required for different pile types of Free-state province of South Africa (b/w Kroonstad and Vredefort)*

| | Rigid Pier | Elastic Straight Shaft Pier | Elastic Belled Pier | Helical Pier |
|---|---|---|---|---|
| Length of Pile Required (m) | 17.83 | 16.8 | 10.36 | 5.6 |

## 5.3. Case Study 3. Compacted expansive soil from Nanning, Guangxi Province in China

Liu et al (2015) made the report however Fan et al. (2007) did a static and immersed pile model test on Nanning expansive soil.

The potential expansiveness of soil was middle swelling grade, low clayey (CL). Jerrican jar has a diameter of 500 mm against a height of 900 mm. 580 mm placement of expansive Nanning soil at the top with 160 mm fine sand in the middle and cobble having 100 mm thickness at the bottom. The pile is PVC pipe having **50 mm diameter, Length of 0.65 m** and filled with fly ash mixture. Allowed movement on top of soil So = 41.2 mm.

Table 14 shows the site data of Nanning, China. Here values from site showing Liquid limit (LL), Plastic limit (PL), Plasticity Index (PI), Specific Gravity, Optimum moisture content (OMC), and Maximum dry density (MDD) are summarized. The active depth is 0.58 m.

*Table 14 Soil data for Nanning, Guangxi Province in China*

| Description | Group Symbol | LL % | PL % | PI % | Specific Gravity | Optimum Moisture Content (%) | Maximum Dry Density (gm/cm3) |
|---|---|---|---|---|---|---|---|
| Montmorillonite dominated clay | CL | 67.5 | 24.5 | 43 | 2.71 | 30 | 1.55 |

**Analytical Result**

Table 15 represents analytical result from Nanning, Guangxi Province in China

*Table 15 Analytical Results for Compacted expansive soil from Nanning, Guangxi Province in China*

| | (Poulos, 1991) | (Silva, 2022) | RSPile | This study |
|---|---|---|---|---|
| Max axial force induced (kN) | 0.14 | 0.42 | 0.42 | 0.63 |
| Max skin friction (kPa) | 1.57 | 2.09 | 4.1 | 6.138 |
| Max net upward movement (mm) | 11.15 | 9.14 | 16.12 | 5.9 |

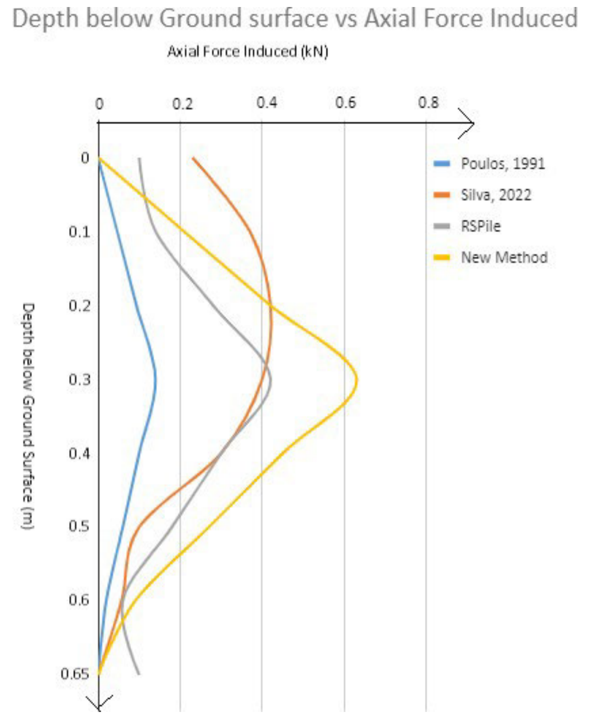


*Figure 17 Chart between Depth below ground surface (GL) vs Axial force induced (kN)*

Figure 17 demonstrates comparison between Depth below ground surface (GL) vs Axial force induced (kN). The site is Nanning, Guangxi Province in China. This study falls close in results as compared to Poulo's Design curve method (1991), Elastic Stress Method using constants of Silva (2022), and RSPile software.

All models describe there is an increase in maximum axial load induced up to active zone depth. The active depth increases from 0 to 0.3 m, the axial force induced also increases from 0 to 0.42 kN (RSPile), 0 to 0.42 kN (Silva, 2022), 0 to 0.14 kN (Poulos, 1991) and 0 to 5.9 kN (This study). The variation between this study with RSPile is 34 %.

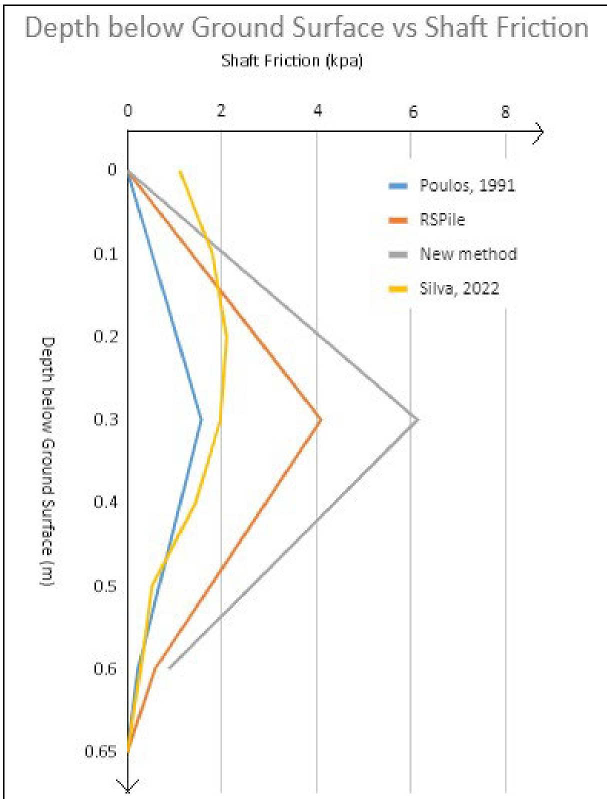


*Figure 18 Chart between Depth below ground surface (GL) vs Skin friction (kPa)*

Figure 18 demonstrates comparison between Depth below ground surface (GL) vs Skin friction (kPa). The site is Nanning, Guangxi Province in China. This study falls close in results as compared to Poulo's Design curve method (1991), Elastic Stress Method using constants of Silva (2022), and RSPile software.

All models describe there is an increase in maximum skin friction on pile-soil interface up to active zone depth. The active depth increases from 0 to 0.3 m, the skin friction also increases from 0 to 4.1 kPa (RSPile), 0 to 2.09 kPa (Silva, 2022), 0 to 1.57 kPa (Poulos, 1991) and 0 to 6.138 kPa (This study). The variation between this study with RSPile is 34 %.

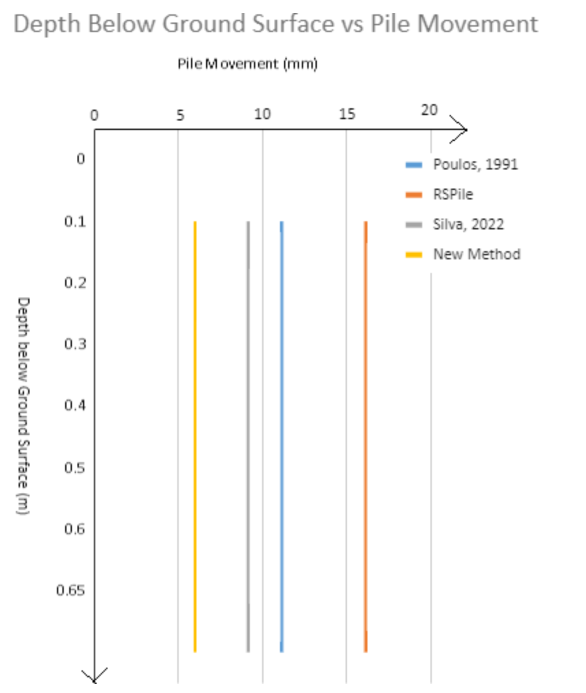


*Figure 19 Chart between Depth below ground surface (GL) vs Soil movement (mm) upward induced*

Figure 19 demonstrates comparison between Depth below ground surface (GL) vs Soil movement (mm) upward induced. The site is Nanning, Guangxi Province in China. This study falls close in results as compared to Poulo's Design curve method (1991), Elastic Stress Method using constants of Silva (2022), and RSPile software.

All models describe there is an increase in maximum net movement in between soil swelling upwards and pile settlement downwards. There is an upward movement which is maximum at ground level at 9.14 mm (RSPile), 16.12 mm (Silva, 2022), 11.15 mm (Poulos, 1991) and 5.99 mm (This study). The variation between this study with RSPile is 174 %.

Chart figures 17, 18, and 19 presents the results of this study, Poulo's Design Curve model, Silva's Method and RSPile's model. Figures demonstrates present model, which is close, implicating that present model can be easily used for estimation of pile-soil interaction in Nanning expansive soil with good level of accuracy compared with those models.

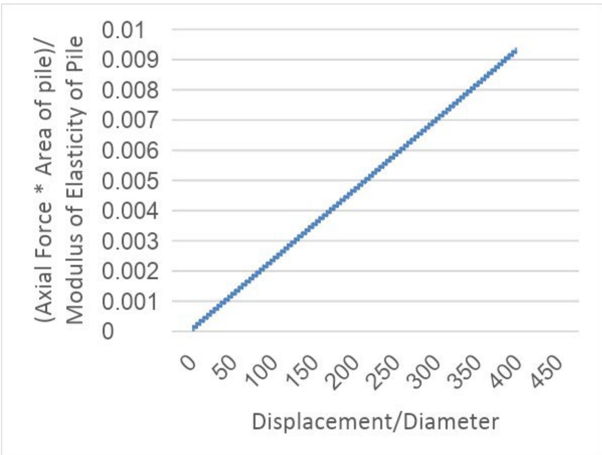


*Figure 20 shows linear relation is established for soil movement against axial force induced in Nanning, Guangxi, China expansive soil site.*

This chart of figure 20 is prepared where vertical axis is $\frac{Axial\ \ Force\ *\ Area\ \ of\ \ pile}{Modulus\ of\ Elasticity\ of\ Pile}$ is put against horizontal axis of $\frac{Displacement\ of\ pile}{Diameter\ of\ pile}$This graph shows a linear relation is established for soil movement against axial force induced in expansive soil without any external dead load applied.

## 5.4. Case Study 4. Shri Vishnu Educational Society, Andhra Pradesh, India

Study was conducted by Gupta (2019) and test soil was collected from Shri Vishnu Educational Society, Bhimacaram, near West Godavari District, Andhra Pradesh, India. Samples were collected from a depth of 5-6 meters depth. Indian Standard classification = CH (high compressible soil, black cotton soil). The diameter of the pile is 500 mm. The length of the pile is 3.6 m. Active depth is 2 m.

Table 16 depicts Soil data from lab for the Shri Vishnu Educational Society, Andhra Pradesh, India. Here results showing Liquid limit (LL), Plastic limit (PL), Plasticity Index (PI), Specific Gravity, Optimum moisture content (OMC), and Maximum dry density (MDD) are summarized.

*Table 16 Soil data from Lab for Shri Vishnu Educational Society, Andhra Pradesh, India*

| Description | Group Symbol | LL % | PL % | PI % | Specific Gravity | Optimum Moisture Content (%) | Maximum Dry Density (gm/cm3) |
|---|---|---|---|---|---|---|---|
| Clay | CH | 70.3 | 27.9 | 42.4 | 2.75 | 28.2 | 1.925 |

**Analytical Result**

Table 17 represents analytical result from Shri Vishnu Educational Society, Andhra Pradesh, India test site.

*Table 17 Analytical Test results of Shri Vishnu Educational Society, Andhra Pradesh, India*

| | (Poulos, 1991) | (Silva, 2022) | RSPile | This study |
|---|---|---|---|---|
| Max axial force induced (kN) | 26.4 | 45.31 | 34.5 | 34.86 |
| Max skin friction (kPa) | 4.67 | 2.09 | 4.1 | 6.138 |
| Max net upward movement (mm) | 14.7 | 16.67 | 16.22 | 14.7 |

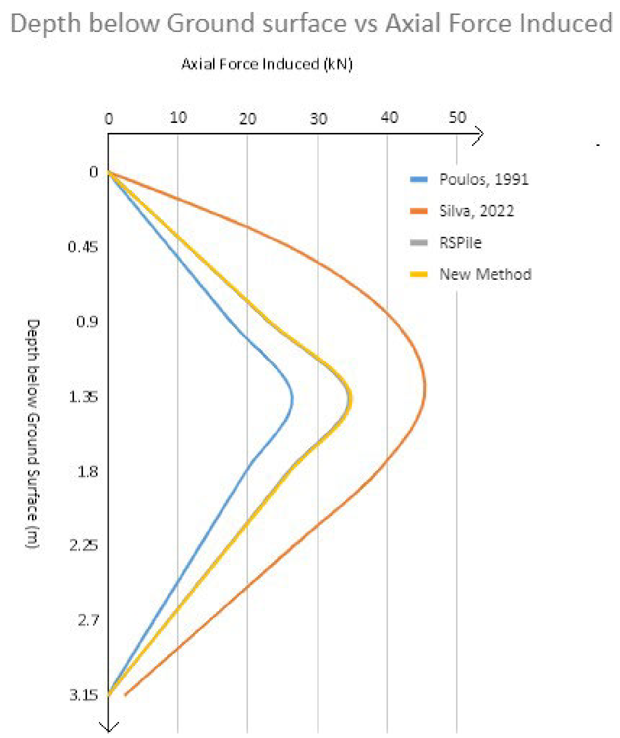


*Figure 21 Chart between Depth below ground surface (GL) vs Axial force induced (kN).*

Figure 21 demonstrates comparison between Depth below ground surface (GL) vs Axial force induced (kN). The site is Shri Vishnu Educational Society, Andhra Pradesh, India test site. This study falls close in results as compared to Poulo's Design curve method (1991), Elastic Stress Method using constants of Silva (2022), and RSPile software.

All models describe there is an increase in maximum axial load induced up to active zone depth. The active depth increases from 0 to 3 m, the axial force induced also increases from 0 to 34.5 kN (RSPile), 0 to 45.31 kN (Silva, 2022), 0 to 26.4 kN (Poulos, 1991) and 0 to 34.86 kN (This study). The variation between this study with RSPile is 2 %.

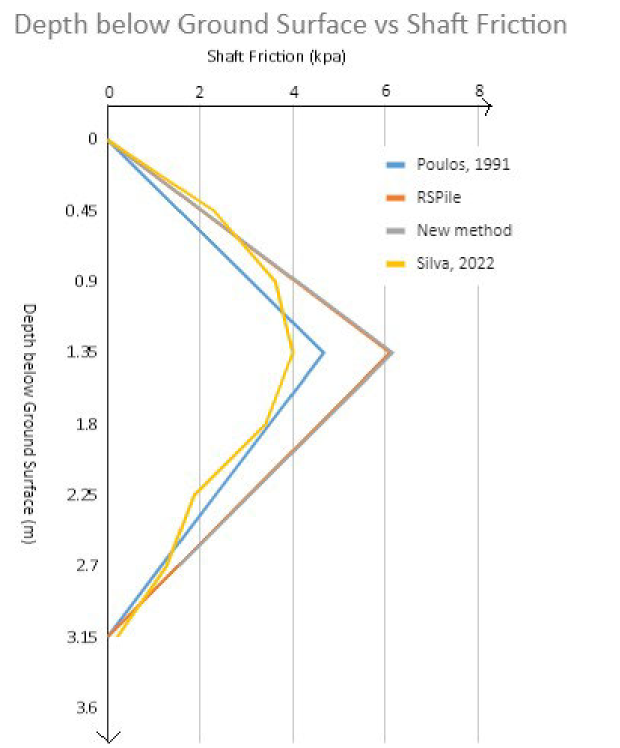


*Figure 22 Chart between Depth below ground surface (GL) vs Skin friction (kPa).*

Figure 22 demonstrates comparison between Depth below ground surface (GL) vs Skin friction (kPa). The site is Shri Vishnu Educational Society, Andhra Pradesh, India test site. This study falls close in results as compared to Poulo's Design curve method (1991), Elastic Stress Method using constants of Silva (2022), and RSPile software.

All models describe there is an increase in maximum skin friction on pile-soil interface up to active zone depth. The active depth increases from 0 to 3 m, the skin friction also increases from 0 to 4.1 kPa (RSPile), 0 to 6.138 kPa (Silva, 2022), 0 to 4.67 kPa (Poulos, 1991) and 0 to 6.138 kPa (This study). The variation between this study with RSPIle is 34 %.

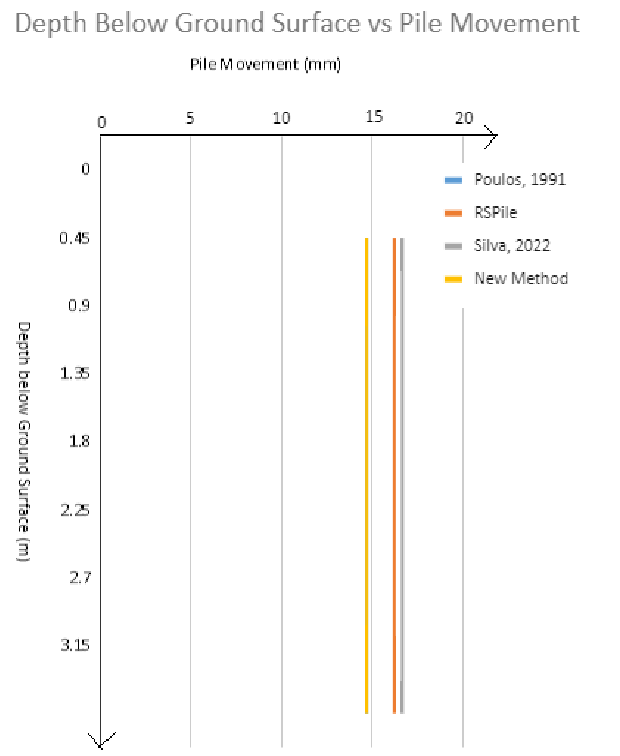


*Figure 23 Chart between Depth below ground surface (GL) vs Soil movement (mm) upward induced*

Figure 23 demonstrates comparison between Depth below ground surface (GL) vs Soil movement (mm) upward induced. The site is Shri Vishnu Educational Society, Andhra Pradesh, India test site. This study falls close in results as compared to Poulo's Design curve method (1991), Elastic Stress Method using constants of Silva (2022), and RSPile software. All models describe there is an increase in maximum net movement in between soil swelling upwards and pile settlement downwards. There is an upward movement which is maximum at ground level at 16.22 mm (RSPile), 16.67 mm (Silva, 2022), 14.7 mm (Poulos, 1991) and 14.7 mm (This study). The variation between this study with RSPile is 11 %.

Figures 21, 22, and 23 presents the results of this study, Poulo's Design Curve model, Silva's Method and RSPile's model. Figure demonstrates present model, which is close, implicating that present model can be easily used for estimation of pile-soil interaction in Colorado expansive soil with good level of accuracy compared with those models.

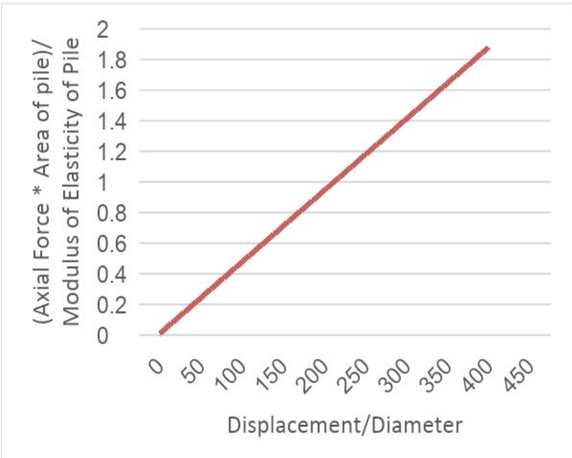


*Figure 24 shows linear relation is established for soil movement against axial force induced in Andhra Pradesh, India expansive soil site.*

This chart of figure 24 is prepared where vertical axis is $\frac{Axial\ Force\ *\ Area\ of\ pile}{Modulus\ of\ Elasticity\ of\ Pile}$ is put against horizontal axis of $\frac{Displacement\ of\ pile}{Diameter\ of\ pile}$ This graph shows a linear relation established for soil movement against axial force induced in expansive soil without any external dead load applied.

# 6. Discussion

### 6.1. Difference in results between this study vs Elastic Solution (Silva, 2022)

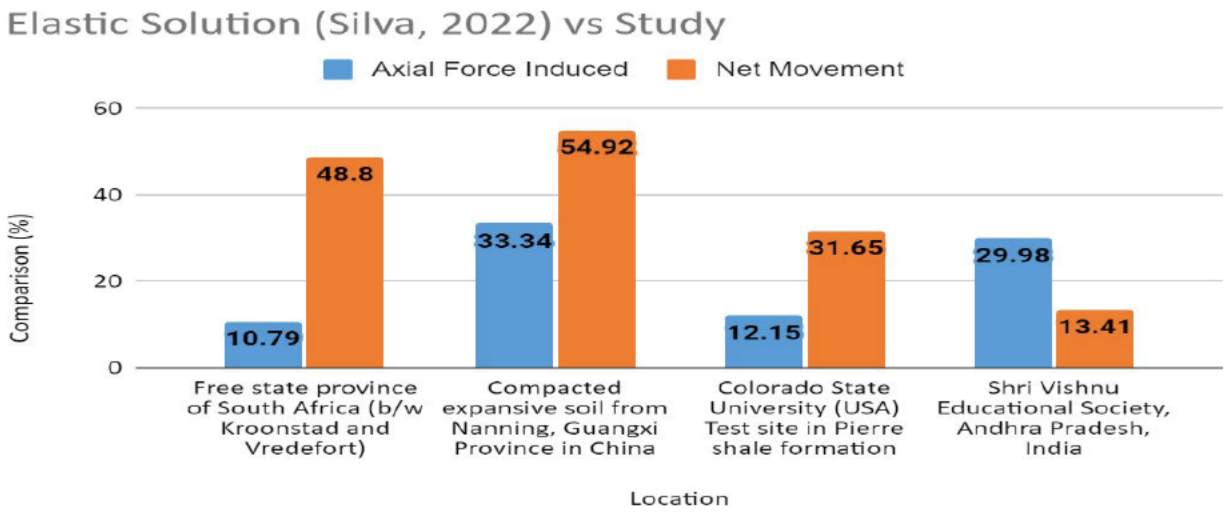


*Figure 25 shows the difference in results between Elastic solution vs this study.*

Figure 25 and table 18 depicts the difference in results between Elastic solution using constants by Silva, 2022 and this study.

*Table 18 shows the difference in results between Elastic solution vs this study.*

| Location | Axial Force | | Error (%) | Net Movement | | Error (%) |
|---|---|---|---|---|---|---|
| | Elastic Solution (kPa) (A) | This Study (kPa) (B) | $\lvert\frac{A-B}{B}\rvert x100$ | Elastic Solution (mm) (A) | This Study (mm) (B) | $\lvert\frac{A-B}{B}\rvert x100$ |
| Free state province of South Africa (b/w Kroonstad and Vredefort) | 628.05 | 566.89 | 10.79 | 12.7 | 24.8 | 48.8 |
| Compacted expansive soil from Nanning, Guangxi Province in China | 0.42 | 0.63 | 33.34 | 9.14 | 5.9 | 54.92 |
| Colorado State University (USA) Test site in Pierre shale formation | 157.73 | 140.65 | 12.15 | 10.8 | 15.8 | 31.65 |
| Shri Vishnu Educational Society, Andhra Pradesh, India | 150.8 | 130 | 16 | 0.7 | 0.3 | 133.34 |

**Discussion**: It can be concluded from these comparison results that this study can give close results to established empirical methods for Colorado and Province site.

### 6.2. Difference in results between this study vs RS Pile Software

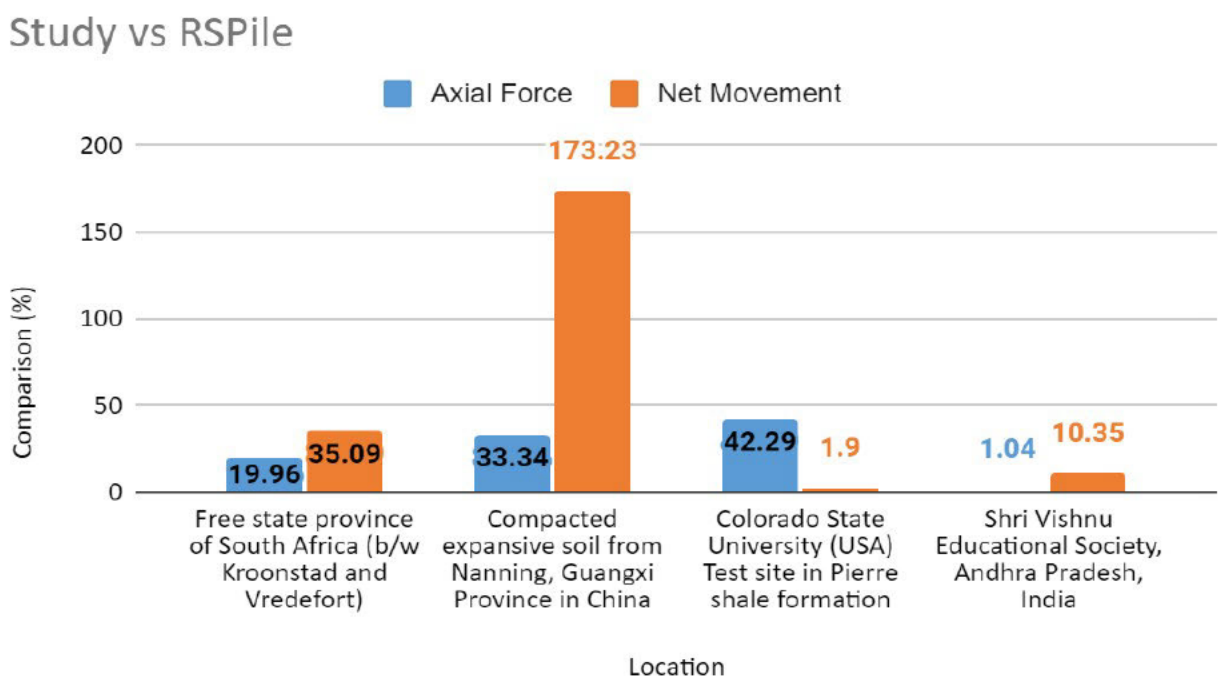


*Figure 26 shows difference in results between this study vs RS Pile software.*

Figure 26 and Table 19 depicts the difference in results between this study vs RS Pile software.

*Table 19 shows difference in results between this study vs RS Pile software.*

| Location | Axial Force | | Error % | Net Movement | | Error % |
|---|---|---|---|---|---|---|
| | RSPile (kPa) (A) | This Study (kPa) (B) | $\lvert\frac{A-B}{B}\rvert x100$ | RSPile (mm) (A) | This Study (mm) (B) | $\lvert\frac{A-B}{B}\rvert x100$ |
| Free state province of South Africa (b/w Kroonstad and Vredefort) | 680 | 566.89 | 19.96 | 16.1 | 24.8 | 35.09 |
| Compacted expansive soil from Nanning, Guangxi Province in China | 0.42 | 0.63 | 33.34 | 16.12 | 5.9 | 173.23 |
| Colorado State University (USA) Test site in Pierre shale formation | 200.12 | 140.65 | 42.29 | 16.1 | 15.8 | 1.9 |
| Shri Vishnu Educational Society, Andhra Pradesh, India | 34.5 | 566.89 | 1.04 | 16.22 | 24.8 | 10.35 |

**Discussion**: It can be concluded from these comparison results that this this study can give close results to established empirical methods for Colorado and Andhra site.

### 6.3. Difference in results between this study vs Design Curve (Poulos, 1991)

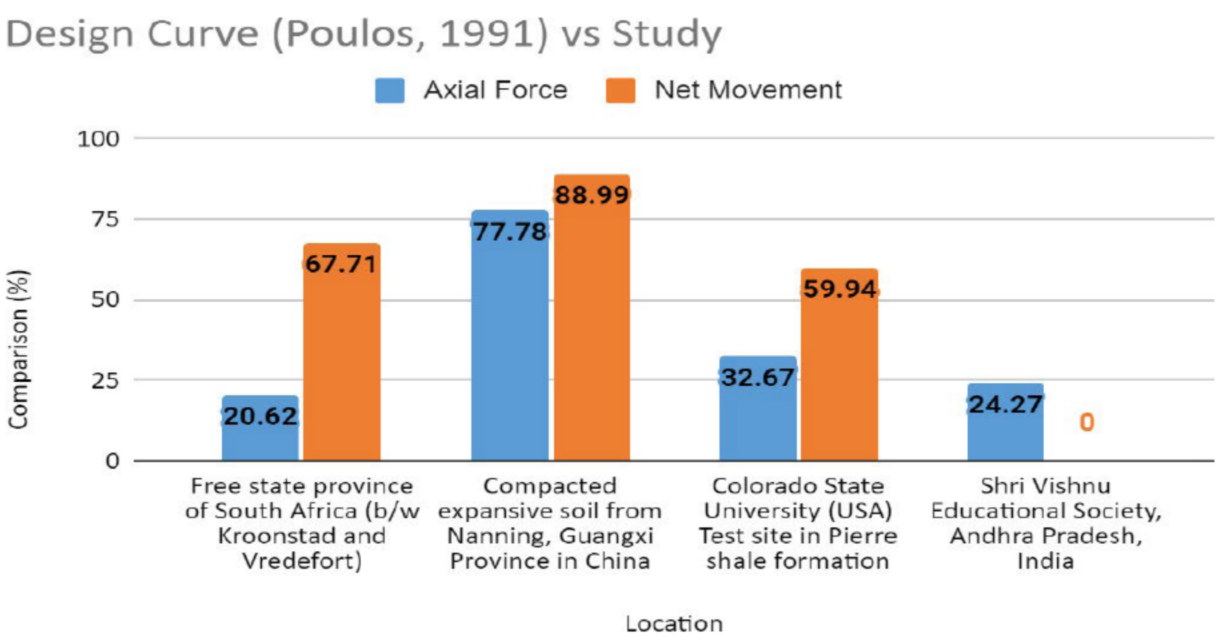


*Figure 27 shows difference in results between this study vs Design Curve by Poulos*

Figure 27 and table 20 depicts the difference in results between this study vs Design Curve (Poulos, 1991).

*Table 20 shows difference in results between this study vs Design Curve by Poulos*

| Location | Axial Force | | Error % | Net Movement | | Error % |
|---|---|---|---|---|---|---|
| | Design Curve (kPa) (A) | This Study (kPa) (B) | $\lvert\frac{A-B}{B}\rvert x100$ | Design Curve (mm) (A) | This Study (mm) (B) | $\lvert\frac{A-B}{B}\rvert x100$ |
| Free state province of South Africa (b/w Kroonstad and Vredefort) | 450 | 566.89 | 20.62 | 8.01 | 24.8 | 67.71 |
| Compacted expansive soil from Nanning, Guangxi Province in China | 0.14 | 0.63 | 77.78 | 11.15 | 5.9 | 88.99 |
| Colorado State University (USA) Test site in Pierre shale formation | 94.7 | 140.65 | 32.67 | 6.33 | 15.8 | 59.94 |
| Shri Vishnu Educational Society, Andhra Pradesh, India | 26.4 | 566.89 | 24.27 | 14.7 | 24.8 | 0 |

**Discussion**: It can be concluded from these comparison results that this this study can give close results to established empirical methods for Colorado, and Andhra site.

### 6.4. Comparison chart - Reduction in Length by different pile types

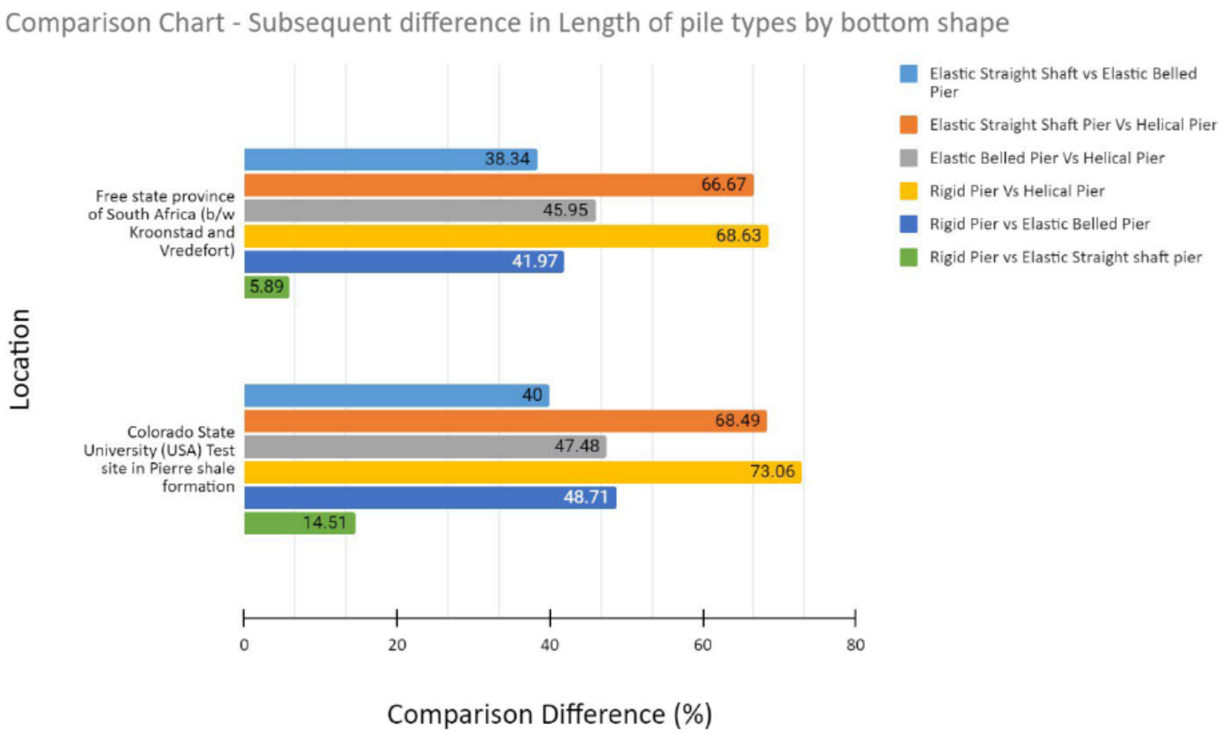


*Figure 28 shows Comparison chart - Reduction in Length by different pile types.*

Figure 28 and table 21 depicts Comparison chart data - Reduction in Length by different pile types. Different pile types and their difference is shown in a single graph. Reduction in length depicts subsequent savings of cost of foundation.

*Table 21 shows Comparison chart data - Reduction in Length by different pile types.*

| Location | Rigid Pier (meters) | Elastic straight shaft pier (meters) | Elastic belled pier (meters) | Helical pier (meters) |
|---|---|---|---|---|
| Free state province of South Africa (b/w Kroonstad and Vredefort) | 17.85 | 16.8 | 10.36 | 5.6 |
| Colorado State University (USA) Test site in Pierre shale formation | 19.3 | 16.5 | 9.9 | 5.2 |

**Discussion**:

1. The maximum pile load is great for short piles however as length gets increased, the maximum load eventually becomes less for same type of pile.
2. In soil zones having high activity or expansive potential i.e., expansive soils using elastic straight shaft pier is not feasible. The usage of belled pier or helical pier is more effective.

# 7. CONCLUSIONS

1. New method gives close results for Colorado site in range of 13-43% error for axial force induced and 2-60% error for net pile movement as shown in discussion section. It gives close results for Province site in range of 11-21% error for axial force induced and 35-68% error for net pile movement.
2. New equation has an advantage as it is developed using suction values as key parameter which can be superimposed using table of Snethen et al (1977) who had established relation between suction and Atterberg limits among other researchers like Nayak and Christensen on Plasticity Index, & Percent Clay (1971), and Yoder & Witczak on percent swell (1975).
3. The new method is easy to implement and require values which can be obtained easily through soil labs like Liquid limit, plastic limit, and Unit weight, etc. or pile data by designer/supplier.
4. RSPile software gives results among axial force and pile movement only in case of axially loaded piles. However, skin friction can be obtained by dividing axial force by surface area.
5. Dimensional modelling methods like Rayleigh is viable tool to derive new equations as it requires least parameters and easy to use. Buckingham's method can also be used however it is only useful when related parameters exceed four in totality.
6. Using relation tables from studies which were conducted for connecting relations by different researcher studies, missing data can be easily acquired by obtaining interconnections between parameters.
7. Elastic solution by Silva's overestimates results and Design Curves by Poulo's give concise results. The difference in results of Poulo's and Silva at Nanning lab site is at 66 %.
8. Huge saving in length is predictable in range close to 73 % when using helical pier as compared to rigid pier. Hence the usage of belled or helical shaped bottom piers is highly effective in sites having high expansive potential thereby saving huge costs for investors.

# 8. FUTURE WORK

1. Due to limitation on time of research. The study only investigated pile-soil interaction under uniaxial loading only. Prospective studies should focus on pile-soil interaction in expansive soil under lateral loading, and with different combinations of loading like snow, etc.
2. Another means of checking the effects of heave is to use finite element method with permutation considering time, ingression of other materials, etc., and comparing with established methods. However, the method is complex and require more research for comparison with this study.

# 9. References


1. A. A. Al-Rawas, I. Guba, and A. Mcgown 1998. *Geological and engineering characteristics of expansive soils and rocks in northern Oman*, Engineering Geology, vol. 50, no. 3-4, pp. 267–281. https://doi.org/10.1016/S0013-7952(98)00023-4.
2. Chengfu Chu, Meihuang Zhan, Qi Feng, Dong Li, Long Xu, Fusheng Zha, Yongfeng Deng 2020. *Effect of Drying-Wetting Cycles on Engineering Properties of Expansive Soils Modified by Industrial Wastes*, Advances in Materials Science and Engineering, vol. 2020, Article ID 5602163, 9 pages. https://doi.org/10.1155/2020/5602163.
3. Elsharief A. M. 1987. *Foundation on Expansive Soils: A laboratory and Field Investigation of Swelling Potential and Performance of Short piles in Expansive Soils*, M.Sc. Thesis in Civil Engineering at Building and Road Research Institute, University of Khartoum. https://www.researchgate.net/publication/302899750_Foundations_on_Expansive_Soils_Sudan_Experience.
4. Chen, F. H. 1988. *Foundations on expansive soils*. Amsterdam; New York : New York, NY, U.S.A: Elsevier; Distributors for the U.S. and Canada, Elsevier Science Pub. Co. https://books.google.com.au/books/about/Foundations_on_expansive_soils.html?id=zdxRAAAAMAAJ&redir_esc=y.
5. Cheng, C.Y., Dasari, G.R., Chow, Y.K., and Leung, C.F. 2007. *Finite element analysis of tunnel–soil–pile interaction using displacement-controlled model*. Tunnelling and underground space technology, 22(4), 450-466. https://doi.org/10.1016/j.tust.2006.08.002.
6. Clayton A. Signor, M.S.E. 2011. *Driven Piles in Central Texas Expansive Soils*. TX Pile, LLC, Austin, Texas, USA. http://hdl.handle.net/2152/ETD-UT-2011-12-4880.
7. Fan, Z.H., Wang, Y.H., Xiao, H.B., and Zhang, C.S. 2007. *Analytical method of load-transfer of single pile under expansive soil swelling*. Journal of Central South University of Technology, 14(4), 575-579. https://doi.org/10.1007/s11771-007-0110-4.
8. Fredlund, M.D., Wilson, G.W., Fredlund, D.G. 2002. *Representation and estimation of the shrinkage curve*, in: Proc., 3rd Int. Conf. on Unsaturated Soils, UNSAT 2002, pp. 145. https://www.researchgate.net/publication/284484931_Representation_and_estimation_of_the_shrinkage_curve.
9. Gupta, Prof. 2019. *Study of Suitable Foundations for Black Cotton Soil*. International Journal for Research in Applied Science and Engineering Technology. 7. 3230-3237. https://doi.org/10.22214/ijraset.2019.5531.

10. Guo, W.D., and Randolph, M. 1997. *Vertical loaded piles in non-homogeneous media.* International Journal for Numerical and Analytical Methods in Geomechanics, 21, 507-532. http://dx.doi.org/10.1002/(SICI)1096-9853(199708)21:8%3C507::AID-NAG888%3E3.0.

11. Houda, G., Tayeb, B. & Yahiaoui, D. 2018. Key parameters influencing performance and failure modes for interaction soil–pile–structure system under lateral loading. Asian J Civ Eng 19, 355–373. https://doi.org/10.1007/s42107-018-0033-4.

12. Jeong, Sangseom & Lee, Jinhyung & Lee, Cheol. 2004. Slip effect at the pile–soil interface on dragload. Computers and Geotechnics. 31. 115-126. https://doi.org/10.1016/j.compgeo.2004.01.009.

13. Liu, J., Xiao, H.B., Tang, J., and Li, Q.S. 2004. *Analysis of load-transfer of single pile in layered soil.* Computers and Geotechnics, 31(2), 127-135. https://doi.org/10.1016/j.compgeo.2004.01.001.

14. Liu Yunlong, Sai Vanapalli 2021. Chapter 18 - *Pile behaviour modelling in unsaturated expansive soils*, Editor(s): Pijush Samui, Sunita Kumari, Vladimir Makarov, Pradeep Kurup, Modelling in Geotechnical Engineering, Academic Press, 2021, Pages 393-427, ISBN 9780128212059. https://doi.org/10.1016/B978-0-12-821205-9.00003-4.

15. Nayak, N.V. Christensen, R.W., 1971. Swelling characteristics of compacted expansive soils. Clays and Minerals, Vol.19, pp.251-261. Nayak Christensen Swelling Characteristics Expansive Soils | PDF | Porosity | Soil (scribd.com)

16. Poulos, H.G., Davis, E.H. 1980. *Pile foundation analysis and design*. John Wiley & Sons. 294-310. Ch 12. https://books.google.com.au/books/about/Pile_Foundation_and_Design.html?id=i9lRAAAAMAAJ&redir_esc=y.

17. Poulos, H.G. 1991. Analysis of Piled Strip Foundations. Comp. Methods & Advances in Geomechs., ed. Beer et al, Balkema, Rotterdam, 1: 183-191. http://pascal-francis.inist.fr/vibad/index.php?action=getRecordDetail&idt=19716763

18. Rocscience, 2022. RSPile Axially Loaded Piles Theory Manual. static. rocscience.cloud/assets/verification-and-theory/RSPile/RSPile-Axially-Loaded-Piles-Theory.pdf

19. Snethen, Donald R. and Johnson, Lawrence D. and Patrick, D. M. 1977. An Evaluation of Expedient Methodology for Identification of Potentially Expansive Soils. An Evaluation of Expedient Methodology for Identification of Potentially Expansive Soils (bts.gov)

20. Tahasildar, Janardhan & Erzin, Yusuf & Rao, Bendadi. 2016. *Development of relationships between swelling and suction properties of expansive soils*. International Journal of Geotechnical Engineering. 1-13. https://doi.org/10.1080/19386362.2016.1250040.

21. T.S. da Silva Burke, S.W. Jacobsz, M.Z.E.B. Elshafie, and A.S. Osman. 2022. *Measurement of pile uplift forces due to soil heave in expansive clays*. *Canadian Geotechnical Journal*. 59(12): 2119-2134. https://doi.org/10.1139/cgj-2021-0079.

22. Vijayavergiya, V.N., and O.I. Ghazzaly. 1973. Prediction of Swelling Potential for Natural Clays. Proceedings of the 3rd International Conference on Expansive Soils, Haifa, Israel, 1, 227–236. https://www.researchgate.net/publication/Identification_and_prediction_of_the_swelling_behavior_of_some_soils_from_the_Tlemcen_region_of_Algeria_A_Djedid_A_Bekkouche_SM_Mamoune_Bulletin_des_Laboratoires_des_Ponts_et_Chaussees_233_69-77

23. Xiao, H.B., Zhang, C.S., Wang, Y.H., and Fan, Z.H. 2011. *Pile-Soil Interaction in Expansive Soil Foundation*: *Analytical Solution and Numerical Simulation*. International Journal of Geomechanics, 11(3), 159-166. https://doi.org/10.1061/(ASCE)GM.1943-5622.0000046.

24. Yoder EJ, Witczak MW 1975. Principles of pavement design, 2nd edn. Wiley, New York. 187-188 Principles of Pavement Design - E. J. Yoder, M. W. Witczak - Google Books

25. Zhang, D.F., Jun, Y., and Shen, Z.P. 2016. *Analytical solutions of pile-soil interaction in expansive soil foundation with expansion rate and stiffness variation along the depth*. 3(3), 86-93. https://doi.org/10.6052/j.issn.1000-4750.2015.04.0279.

# 10. APPENDICES

## Appendix A – Derivation of new equation

1. Derivation of new equation for pile movement by swelling without loading using soil suction.

S = Soil Suction = kPa or $kN/mm^2$ $\quad M L^{-1} T^{-2}$

P = Perimeter of Pile = $\pi d$ or m $\quad L$

L = Length of Pile = m $\quad L$

K = Stiffness of Pile material = N/m $\quad M T^{-2}$

Using Rayleigh Method

$$L = [M L^{-1} T^{-2}]^a \; [L]^b \; [L]^c \; [$$

For M $\quad 0 = a + d$

For L $\quad 1 = -a + b + c$

For T $\quad 0 = -2a - 2d$

$$a = -d \text{ or } d = -a$$

$$b = 1 - c + a$$

$$c = 1 - b + a$$

$$L = (S)^a \, (L)^{1-c+a}$$

$$L = (LP)^1 \Bigl(SL$$

Simplifying

# Appendix B - Empirical Methods and their design steps

1. Poulo's Method (1980)

***Axial Load Calculation***

$\tau_{am}$ is pile-soil adhesion at the level of pile tip. The maximum pile load, Pmax, is given as a ratio of the load $P_{fs}$ that occurs if full adhesion was mobilized along the whole shaft.

$$P_{fs} = \int_{0'}^{L} \tau \quad \pi \, d \, d_{z} \tag{1}$$

***Load transfer to Pile Tip***

The load proportion, which is being transferred to pile tip, $\beta$ is expressed as $\beta o$ for an incompressible floating pile in semi-finite mass, multiplied by the correction factor to consider the compressibility of the pile and relative stiffness of the bearing load stratum. Please refer appendix for Curves.

$$\beta = \beta_o \, C_k \, C_v \tag{2}$$

where $\beta = \frac{Pb}{P}$ = applied load proportion transferred to pile tip

$\beta_o$ = proportion of tip-load for pile (incompressible) in uniform half-space (Poisson's ratio = 0.5)

$C_k$ = pile compressibility correction factor

$C_v$ = Poisson's ratio of soil correction factor

1. The proportion of load being transferred to pile tip, $\beta$, needed Correction Factor

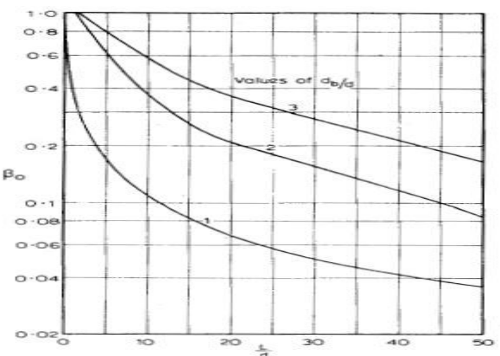


Proportion of base load, $\beta o$

Figure depicts tip-load proportion for incompressible pile in uniform half-space. The presence of an enlarged base increase $\beta$ significantly, $\beta$ being not significantly affected if pile is situated in finite layer rather than a half-space, provided hard base of layer is more than 0.2L below bottom of the pile.

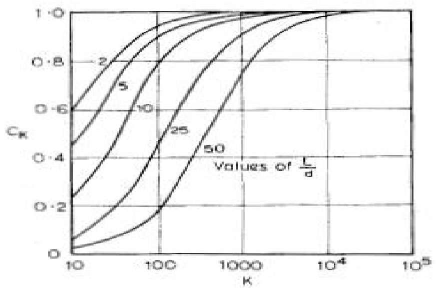


Compressibility correction factor for base load, Ck

Figure depicts correction factor for pile compressibility, Ck, to decrease the amount of load transferred to tip, less than 1.

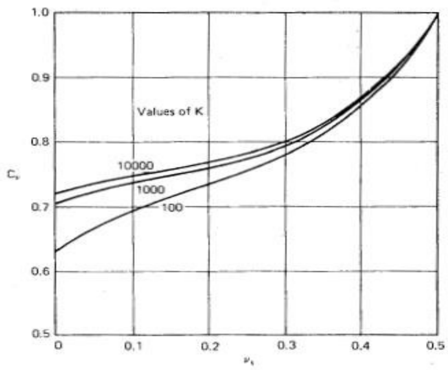


Poisson's ratio correction factor for base load, Cv

Figure depicts correction factor for Poisson's ratio of soil, Cv.

***Settlement of Pile***

The settlement of the top of pile is expressed in terms of incompressible pile in a half-space, with correction factors for the effects of pile compressibility.

$$\rho = \frac{P_u I}{E_s D} \qquad (3)$$

where, $P_u$ = axial force induced (kN)

$\rho$ = axial movement (m)

$E_s$ = modulus of elasticity of soil (MPa)

D = diameter of pile (m)

L = length of pile

$$I = I_o R_k R_b R_v \qquad (4)$$

$I_o$ = settlement-influence factor for incompressible pile in semi-infinite mass, for Poisson's ratio $v_s$ = 0.5

$R_k$ = correction factor for pile compressibility

$R_b$ = correction factor for bearing stratum stiffness

$R_v$ = correction factor for settlement

1. Settlement Influence Charts and Constants

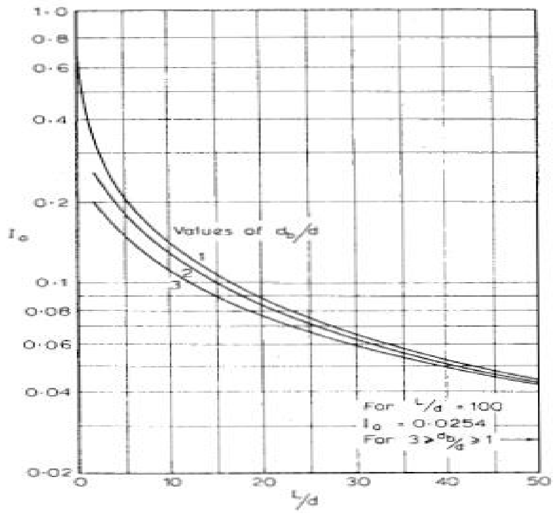


Settlement influence factor, Io

Figure shows decreasing settlement of a pile of constant diameter as length increases. The presence of enlarged base also decreases settlement, although the effect is only significant for short pile. Settlement-influence factor, Io.

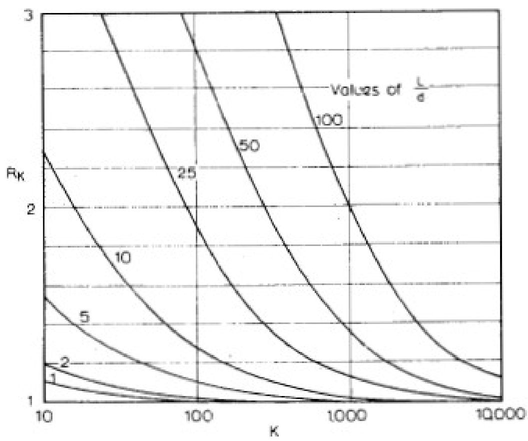


Compressibility correction factor for settlement, Rk

Figure depicts Pile compressibility, Rk, which increases settlement, especially for slender pile.

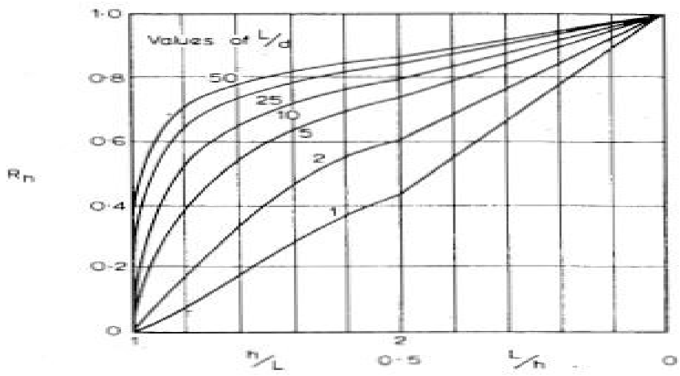


Depth correction factor for settlement, Rh

Figure depicts effect of having a finite layer to decrease settlement.

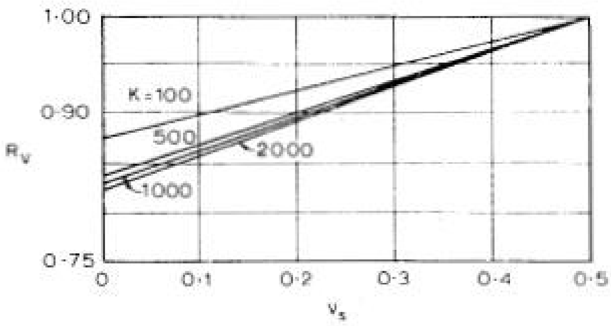


Poisson's ratio correction factor for settlement, Rv

Figure depicts a decrease in Poisson's ratio, vs, while maintaining Es constant leads to a decrease in settlement

For Total Tension induced in pile for Full Length

For estimation of Movement for a pile and maximum pile load for a swelling-soil profile, estimation is done using dimensionless curves. Consideration has been given for both, a constantly increasing pile-soil shear strength, $\tau a$ and linearly increasing $\tau a$ with depth.

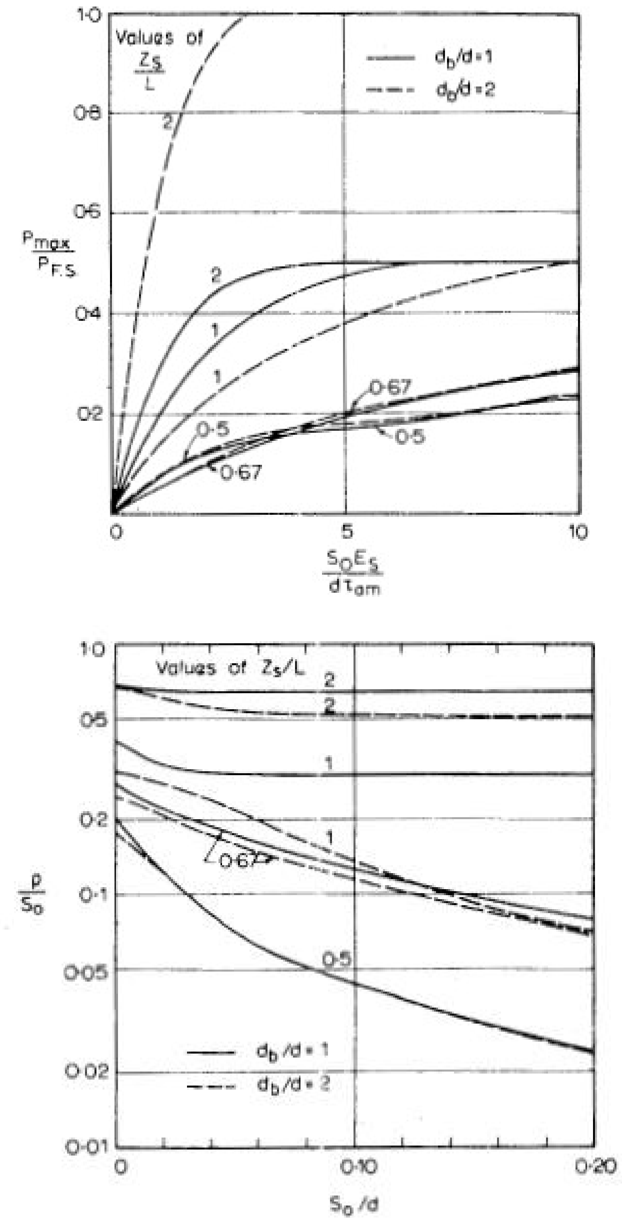


Maximum pile load in swelling soil (a). Pile movement in swelling soil (b). Pile-soil shear strength is linearly increasing with depth.

Graphical figure (a) above depicts maximum pile load in swelling soil. figure (b) depicts soil movement in swelling soil. Pile-soil shear strength is linearly increasing with depth, as a function of dimensionless maximum soil-movement, $\frac{So\ Es}{d\tau am}$ and the dimensionless depth of swelling, $\frac{Zs}{l}$

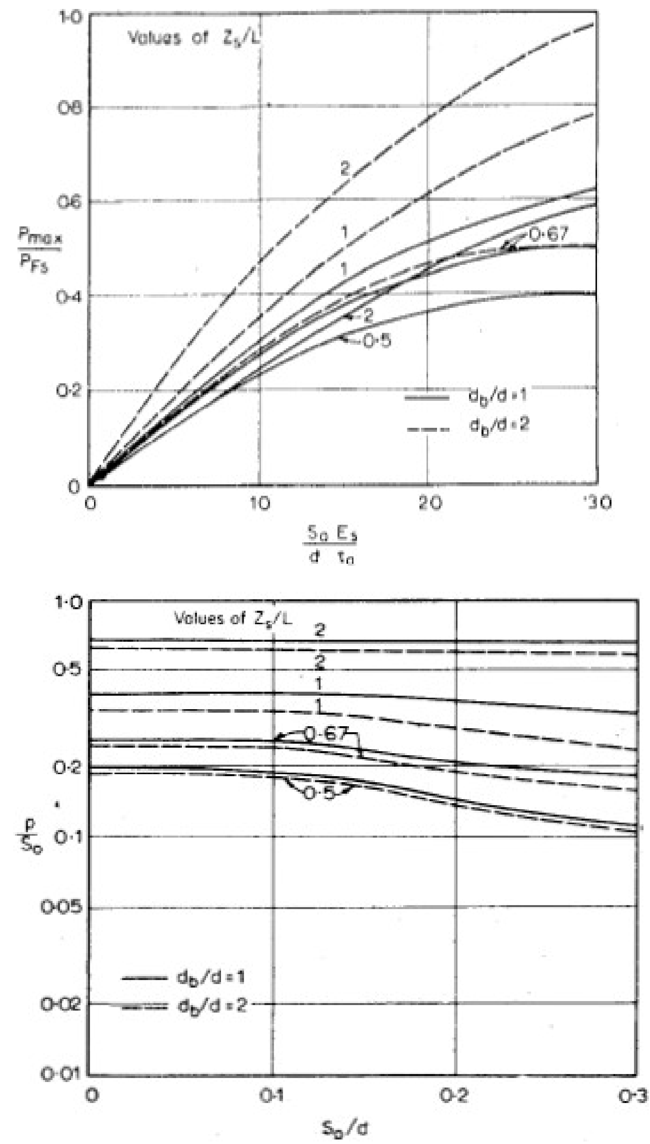


Maximum pile load in swelling soil (a). Pile movement in swelling soil (b). Pile-soil shear strength is constant with depth.

Graphical figure (a) depicts maximum pile load in swelling soil. figure (b) depicts soil movement in swelling soil. Pile-soil shear strength $\tau a$ is constantly increasing with depth, as a function of dimensionless maximum soil-movement, $\frac{So\ Es}{d\tau am}$ and the dimensionless depth of swelling, $\frac{Zs}{l}$.

Net movement = $\rho - w_p$ (5)

2. Elastic Method using Silva's Design Constant - Step

| | |
|---|---|
| C3 | $\frac{-S_o}{\alpha\, h_o}$ |
| C4 | $C6\ +\ \frac{s_o\, sinh\,(\alpha\, h_o)}{\alpha\, h_o}$ |
| C5 | $C3\ +\ \frac{s_o\, cosh\,(\alpha\, h_o)}{\alpha\, h_o}$ |
| C6 | $\frac{-cosh\,(\alpha L)}{sinh\,(\alpha L)} C5 = \frac{-\, s_o\, cosh\,(\alpha L)\,(cosh\,(\alpha\, h_o) - 1)}{\alpha\, h_o\, sinh\,(\alpha L)}$ |

w is soil movement in meters and P is axial uplift force.

a. $E_p$ = modulus of elasticity of pile, $A_p$ is the cross-sectional surface area of the pile,

b. $\alpha^2\ =\ \frac{2\,\pi}{\lambda_p\, A_p\, \varsigma}$ (6)

c. $\varsigma$ = ln $(\frac{r_m}{r_o})$ (7)

d. $r_m$ = 2.5 L (1-v) (8)

e. $\lambda\ =\ \frac{E_p}{G_s}$ (9)

We will be using constants by Silva for calculation.

$$w1\,(z)\ =\ C3\, sinh\,(\alpha z)\ +\ C4\, cosh\,(\alpha z)\ -\ \frac{s_o\,(h_o - z)}{h_o};\ 0 \le z \le h_o \quad (10)$$

$$w2\,(z)\ =\ C5\, sinh\,(\alpha z)\ +\ C6\, cosh\,(\alpha z);\ h_o \le z \le L \quad (11)$$

$$P1\,(z)\ =\ -E_p A_p\ (\alpha\, C3\, cosh\,(\alpha z)\ +\ \alpha\, C4\, sinh\,(\alpha z)\ +\ \frac{s}{h_o});\ 0 \le z \le h_o \quad (12)$$

$$P2\,(z)\ =\ -E_p A_p\ (\alpha\, C5\, cosh\,(\alpha z)\ +\ \alpha\, C6\, sinh\,(\alpha z)\,);\ h_o \le z \le L \quad (13)$$

3. Pile Design by Nelson's Approach

1. Relationship between overburden, swelling and inundation pressure is calculated for solving different parameters.

$$\sigma'_{cv} = \sigma'_i + (\sigma'_{cs} - \sigma'_i) \quad (20)$$

$\sigma'_{cv}$ = overburden pressure (kPa)

$\lambda$ = constant depending upon mineralogy of clay soil

$\sigma'_{cs}$ = swelling pressure (kPa) obtained from Consolidation swell data from site

$\sigma'_i$ = inundation pressure (kPa) obtained from Consolidation swell data from site

2. Determination of Heave Index, $C_H$

$$C_H = \frac{\%S_A}{log\sigma'_{cv} - log(\sigma'_i)_A} \quad (21)$$

$\%S_A$ = Percent Swell obtained from Consolidation swell data from site

3. Potential heave depth, $z_p$, is calculated by equating overburden pressure to swelling pressure.

$$(\delta * \omega * L) + (\delta * \omega * (z_p - L) = \sigma'_{cv} \quad (22)$$

$\delta$ = total density of soil from site

$\omega$ = standard water density

4. For the heave calculation of soil, the profile is divided into several n layers of thickness, z.

$$\sigma'_{vo} = \delta * \omega * z \quad (23)$$

$\sigma'_{vo}$ = Effective Stress at depth, z

5. The heave, $\rho$, at every n depth, z, is calculated and summed up to predict total heave. A profile is prepared for a free-field profile.

$$\rho = \sum_1^n [\frac{C_H z_i}{(1+e_0)} log(\frac{\sigma'_f}{\sigma'_{cv}} \quad (24)$$

where: $\rho$ = free-field heave

$C_H$ = heave index

$\sigma'_f$ = final effective stress state

$\sigma'_{cv}$ = swelling pressure from constant volume oedometer test

$e_0$ = initial void ratio

$z_i$ = layer thickness

6. uplift skin friction force

$$F_u = \alpha_1 \, \sigma'_{cv} \, z_p \, \pi \, d \tag{25}$$

$\alpha_1$ = coefficient of uplift between pier and soil; assumed between 0.1 and 0.25 (Nelson and Miller, 1992)

negative (anchorage) skin friction force

$$F_s = \alpha_2 \sigma'_h \, (L - z_p) \, \pi \, d \tag{26}$$

$\alpha_2$ = coefficient of negative friction between pier and soil; assumed between 0.1 and 0.25 and higher than uplift coefficient (Nelson and Miller, 1992)

$\sigma'_h$ = lateral stress acting on pier in anchorage zone

7. Summation of both uplift and negative skin friction force with dead load for finding required length of pile.

The resistance to uplift ($P_r$) is offered by the adhesion resistance for the pile ($L - z_a$) and the allowable dead load from superstructure. Safe design requires uplift force be less than or equal to withholding force or Resistance (W)

$P_r$ = Resistive force on pier (kN)

$\alpha$ = adhesion between clay and pier (kPa)

$Z$ = Total Length of Pier (m) = $Z_a + Z_{na}$

$Z_a$ = Active zone depth (m) (27)

$Z_{na}$ = length extending beyond active zone (m)

$P_r$ = $(\alpha * \pi D * Z_{na})$ + (Dead Load kN) (28)

Equating (1) and (2), required total length of rigid pier is obtained.

**3.1. For the design of an elastic straight shaft pier**

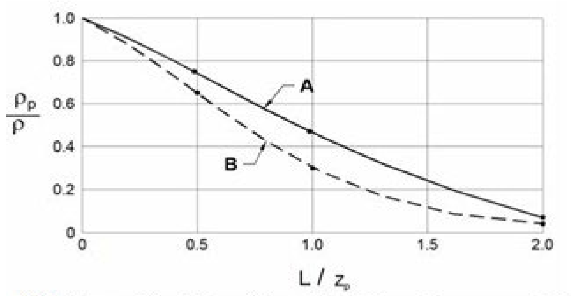


(a) Normalized Straight Shaft Pier Heave vs. L/$z_p$.

*Figure shows normalized straight shaft pier heave vs L/zp. (Nelsons 2007)*

Figure 7 shows normalized straight shaft pier heave vs $L/z_p$ . Getting $\frac{\rho_p}{\rho}$ and intersecting against Curve A can be used for deriving length required for elastic straight shaft pier. (Nelsons 2007)

### 3.2. For the design of the Belled pier Design,

The design of the bell at the bottom provides additional resistance.

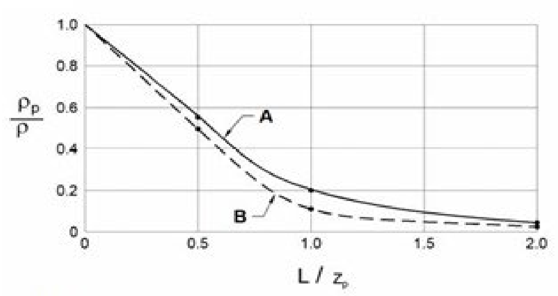


(a) Normalized Belled Pier Heave vs. $L/z_p$.

*Figure shows normalized Belled pier heave vs L/zp. (Nelsons 2007)*

Figure 8 shows normalized belled pier heave vs $L/z_p$ . Getting $\frac{\rho_p}{\rho}$ and intersecting against Curve A can be used for deriving length required for belled pier.

### 3.3. For the design of the Helical Pier Design

Free field heave profile is generated for each depth increment and solved for the depth of the pier by checking against pier movement. The graphical profile generated for free-field heave is checked and the length of the pier is selected based on heave movement on the amount of movement to restrict.

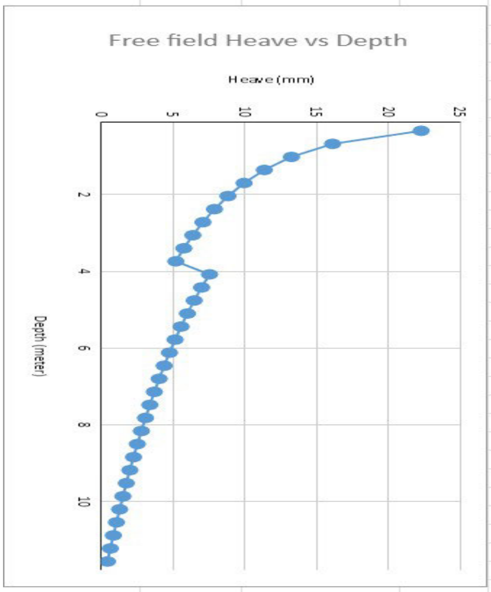


| | | | $\sigma'_{cv} = \sigma'_i + \lambda(\sigma'_{cs} - \sigma'_i)$ | $\rho = C_H \cdot \Delta z \log\left[\frac{\sigma'_{cv}}{(\sigma'_{cs})_z}\right]$ | |
|---|---|---|---|---|---|
| Layer | Depth (m) | Mid (mm) | Stress (kPa) | Heave in Layers (mm) | Cumulative Heave (mm) |
| 1 | 0.34 | 0.17 | 3.068568 | 22.29713448 | 22.29713448 |
| 2 | 0.68 | 0.51 | 9.205704 | 16.13272787 | 38.42986235 |
| 3 | 1.02 | 0.85 | 15.34284 | 13.26644203 | 51.69630438 |
| 4 | 1.36 | 1.19 | 21.479976 | 11.37846781 | 63.07477218 |
| 5 | 1.7 | 1.53 | 27.617112 | 9.96832126 | 73.04309345 |
| 6 | 2.04 | 1.87 | 33.754248 | 8.84234099 | 81.88543444 |
| 7 | 2.38 | 2.21 | 39.891384 | 7.90498637 | 89.79042081 |
| 8 | 2.72 | 2.55 | 46.02852 | 7.102035415 | 96.89245622 |
| 9 | 3.06 | 2.89 | 52.165656 | 6.399734418 | 103.2921906 |
| 10 | 3.4 | 3.23 | 58.302792 | 5.775637958 | 109.0678286 |
| 11 | 3.74 | 3.57 | 64.439928 | 5.214061194 | 114.2818898 |
| 12 | 4.08 | 3.91 | 70.577064 | 7.560552021 | 121.8424418 |
| 13 | 4.42 | 4.25 | 76.7142 | 7.006505779 | 128.8489476 |
| 14 | 4.76 | 4.59 | 82.851336 | 6.49512232 | 135.3440699 |
| 15 | 5.1 | 4.93 | 88.988472 | 6.020298544 | 141.3643685 |
| 16 | 5.44 | 5.27 | 95.125608 | 5.577153996 | 146.9415225 |
| 17 | 5.78 | 5.61 | 101.262744 | 5.161724632 | 152.1032471 |
| 18 | 6.12 | 5.95 | 107.39988 | 4.770746833 | 156.8739939 |
| 19 | 6.46 | 6.29 | 113.537016 | 4.401501534 | 161.2754955 |
| 20 | 6.8 | 6.63 | 119.674152 | 4.051699424 | 165.3271949 |
| 21 | 7.14 | 6.97 | 125.811288 | 3.719394904 | 169.0465898 |
| 22 | 7.48 | 7.31 | 131.948424 | 3.402920542 | 172.4495103 |
| 23 | 7.82 | 7.65 | 138.08556 | 3.100836451 | 175.5503468 |
| 24 | 8.16 | 7.99 | 144.222696 | 2.811890685 | 178.3622375 |
| 25 | 8.5 | 8.33 | 150.359832 | 2.534987887 | 180.8972253 |
| 26 | 8.84 | 8.67 | 156.496968 | 2.269164218 | 183.1663896 |
| 27 | 9.18 | 9.01 | 162.634104 | 2.013567107 | 185.1799567 |
| 28 | 9.52 | 9.35 | 168.77124 | 1.767438763 | 186.9473954 |
| 29 | 9.86 | 9.69 | 174.908376 | 1.53010262 | 188.4774981 |
| 30 | 10.2 | 10.03 | 181.045512 | 1.300952134 | 189.7784502 |
| 31 | 10.54 | 10.37 | 187.182648 | 1.079441436 | 190.8578916 |
| 32 | 10.88 | 10.71 | 193.319784 | 0.8650775052 | 191.7229691 |
| 33 | 11.22 | 11.05 | 199.45692 | 0.6574135552 | 192.3803827 |
| 34 | 11.56 | 11.39 | 205.594056 | 0.4560434306 | 192.8364261 |
| | | | | 193 | |

*Figure free-field heave profile for Colorado by adding or cumulating heave at each layer*

## Appendix C – Design of Length of foundation pier by different bottom types

1. Design of Length of pier for Colorado Site

Foundation design

1. Swelling pressure for constant volume

$\sigma'_{cv} = 48 + 0.6 \times (240 - 48) = 163\ kPa$ for Clay

$\sigma'_{cv} = 48 + 0.6 \times (335 - 48) = 220\ kPa$ for claystone

2. Heave Index

$C_H = 2\% / \log(163/48) = 0.038$ for clay

$C_H = 3\% / \log(220/48) = 0.045$ for claystone

3. Depth of Potential heave, $z_p$

$(1.84 \times 9.81 \times 3) + [1.94 \times 9.81 \times (z_p - 3)] = 220\ kPa$

$z_p = 11.7\ m$

Soil is divided into 35 layers

Each layer $= 11.7/35 = 0.33\ m$ thick

Mid point of first layer $= 0.17\ m$ below GL

4. Effective stress at 1st depth

$\sigma'_{vo} = 1.84 \times 9.81 \times 0.17 = 3.1\ kPa$

Heave of layer

$\rho_1 = 0.038 \times 0.33 \times \log(163/3.1) = 0.022\ m = 22\ mm$

Using Spreadsheet, all depths are calculated & added.

Total free-field heave is 193mm

5. Uplift skin friction

$F_{u1} = \alpha_1 \sigma'_{cv} z_p \pi d$

$= 0.2 \times 163 \times 3 \times \pi \times \frac{254}{1000} = 78\ kN$ from Clay

~~Negative (anchorage) skin friction~~

$F_{u2} = 0.2 \times 220 \times (11.7 - 3) \times \pi \times \frac{254}{1000} = 305\ kN$ from claystone

Total $F_u = 383\ kN$

$\alpha_s$ is taken as 0.25

$F_s = f_s (L - z_p) \pi d$

$= (0.25 \times 220) \times (L - 11.7) \pi (254/1000)$

$= 43.9L - 513.6\ kN$

Summing all loads

$43.9L - 513.6 + 50 = 383\ kN$

$L_{reqd} = 19.3$ metres

6. Using figure
required length of an elastic straight shaft pier with 50 mm of movement
$\rho_p/\rho = 50/193 = 0.26$
$L/z_p = 1.43$
Depth of Potential heave $= 11.7$ m
$L_{reqd} = 1.43 \times 11.7 = 16.7$ meters

7. Using figure
required length of an elastic belled pier with 50 mm of movement
$L/z_p = 0.85$ for $\rho_p/\rho = 50/193 = 0.26$
$L_{reqd} = 0.85 \times 11.7 = 9.9$ meters

8.

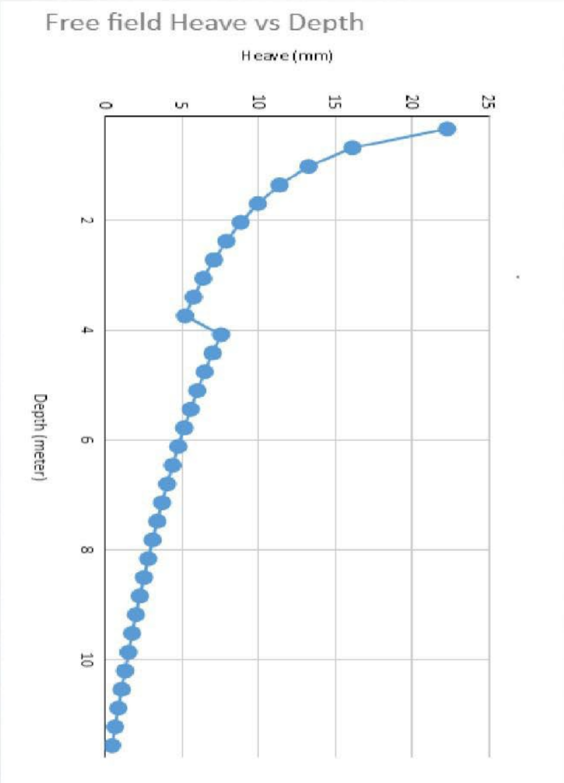


For 50 mm of movement
Required length is 5.2m
for a helical pier

2. Design of Length of pier for Province Site

| Oedometer data | | | | | Consolidation-Swell Test Inundation pressure = 45 kPa | |
|---|---|---|---|---|---|---|
| Soil Type | Height (m) | Water Content (%) | Expansive Potential | Total Density (Mg/m3) | Percent Swell (%) | Swelling Pressure (kPa) |
| Native Clay | 7 | 12.8 | 1.1 | 1.76 | 8.0 | 139 |

Using spreadsheet, all heaves are summed up.
Total free-field heave is 229 mm

5. Uplift Skin friction

$f_{u_1} = \alpha_1 \sigma'_{cv} z_p \pi d$

$= 405.9$ KN

Total $F_u = 405.9$ KN

$\alpha_s$ is taken as 0.25

$F_s = f_s (L - z_p) \pi d$

$= 0.25 \times 102.6 \times (L - 12.95) \times \pi \times 0.9$

$= 72.53L - 939.18$

Summing all loads

$72.53L - 939.18 + 50 = 405.9$ KN

Length of Rigid Pile required = 17.85 m

6. Using figure

required length of an elastic straight shaft pier with 50 mm of movement

$\rho_p / \rho = 50/229 = 0.218$

$L/z_p = 1.3$

Depth of potential heave, 12.95 m

$L = 16.83$ m

7. Using figure

required length of a elastic belled pier with 50 mm of movement

$\rho_p/\rho = 50/229 = 0.218$

$L/z_p = 0.8$

Depth of potential heave, $z_p = 12.95$ m

$L_{reqd} = 10.36$ m

8. Helical pier

For 50 mm of movement

required length is 5.6m for a helical pier

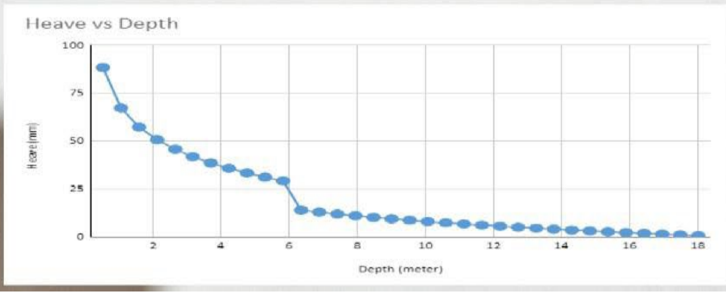

## Appendix D – Analytical Results from – Poulo’s, and Present study

1. Pic showing Poulos results for Colorado.

Colorado

PI = 18

LL = 40

Diameter of pile = 0.254m

Specific Gravity = 2.65

Length of Pile = 19.3m

Surface swell, $S_0$ = 50 mm

Active depth, $h_0$ = 7 m

Poisson's ratio, $\nu$ = 0.3

Modulus of Elasticity of Pile = 32.5 GPa

Modulus of Elasticity of Soil = 16.8 MPa

Friction angle = 30° (of soil)

Horizontal Earth pressure coefficient, k = 0.6

Unit weight of soil, $\gamma$ = 16.9 kN/m³

Dead load application = 50 kN

1) Poulo's

a) Zero Axial loading

$$P_{FS} = \int_0^L \tau_a \pi d \, dz$$

$$\tau_a = k \gamma h \tan\phi$$

$$= 0.6 \times 16.9 \times 7 \times \tan 30^\circ$$

$$= 40.9 \text{ kN/m}^2$$

$$P_{FS} = 1.7 \times \pi \times 0.254 \times 19.3$$

$$= 632 \text{ kN}$$

Using fig 12.16

for $d_b/d = 1$, $z_s/L = 7/19.3 = 0.36$

$$\& \left(\frac{S_0}{d}\right)\left(\frac{E_s}{\tau_a}\right) = 1900$$

$$\frac{P_{max}}{P_{FS}} = 0.3$$

from fig 12.17

$$z_s / L = 0.36 \qquad \frac{S_o}{d} = \frac{0.05}{0.254} = 0.2$$

$$\frac{\rho}{S_o} = 0.15 \qquad \rho = 7.5\,mm \text{ (upwards)}$$

b) Axial load of 50 kN

$$\beta = \beta_o C_K C_v$$

$$K = \frac{E_p}{E_s} = 1600$$

$$L/d = \frac{19.3}{0.25} = 77.2$$

from fig 5.11, 5.12 & 5.13

$$\beta = 0.078$$

Base load $= \beta \times P_{max} = 189.36 \times 0.078 = 14.768$

Using Fig 12.8 from Poulos, Max tensile force occurs at 0.5 L or 9.7 m. Here applied load causes an axial force of ~~[illegible]~~ 94.7 kN

→ Thus net tensile force $(94.7 - 94.7) = 94.7$ kN

Now axial movement caused by applied loading

$$\rho = \frac{P I}{d E_s}$$

Using fig 5.18 to 5.21 $I = 0.108$ (from Poulos)

$$\rho = \frac{50000 \times 0.108}{0.25 \times 16.8 \times 10^6} = 1.2\,mm \text{ (downward)}$$

→ Net movement caused by axial loading & swelling

$$1.2 - 7.5 = 6.3\,mm \text{ (upward)}$$

→ Skin friction $= \frac{94.7}{\pi \times 0.25 \times 19.3} = \cancel{120.535\ kPa}\ 6.25\ kN/m^2$

2. Pic showing Study results for Colorado.

2) Present Study

Stiffness of Pile $= \frac{AE}{L} = \frac{\frac{\pi}{4} \times 0.254^2 \times \overset{26.5}{\cancel{32.5}} \times 10^9}{19.3}$

$= 82660104.63 \text{ N/m}$

Using PI values from study

Suction values is obtained from table by Snethen et al (1977)

$S_u = 97 \text{ kPa}$

a) Pile movement by swelling

$w_s = \frac{S_u P L}{k} = \frac{97 \times 10^3 \times \pi \times 0.254 \times 19.3}{82660104.63}$

$= 17 \text{ mm}$ (upward)

b) Pile movement by 50 kN Loading

$I = 0.108$ (from previous Poulos)

$\rho = \frac{50000 \times 0.108}{0.25 \times 16.8 \times 10^6} = 1.2 \text{ mm}$ (downward)

Net movement caused by axial loading and swelling

$1.2 - 17 = 15.8 \text{ mm}$ (upward net movement)

Max Skin friction $= 0.5(2c'H + K_0 \gamma H^2 \tan\phi)$

$= 9.25 \text{ kN/m}^2$

Max Uplift Force

$=$ Max Skin friction $\times \pi d l$

$= 140.65 \text{ kN}$

3. Pic showing the Poulos results for Province.

Free State Province

$PI = 41$

$LL = 62$

Diameter of Pile = 0.9 m

Specific Gravity = 2.65

Length of Pile = 17.85

Surface Swell, $S_o$ = 56 mm

Active depth, $h_o$ = 7 m

Poisson's ratio, $v$ = 0.3

Modulus of Elasticity of Pile = 21.5 GPa

Modulus of Elasticity of Soil = 15.2 MPa

Friction Angle = 30° (of Soil)

Horizontal earth pressure coefficient, $k = 0.6$

Unit weight of soil, $\gamma = 19.5 \ kN/m^3$

Dead load applied = 50kN

1) Poulos

a) zero Axial load

$$P_{FS} = \int_0^L \tau_a \pi d \, dz$$

Here $\tau_a = k \gamma h \tan\phi$

$$= 0.6 \times 19.5 \times 7 \times \tan 30° = 47.3 \ kN/m^2$$

$$P_{FS} = 47.3 \times \pi \times 0.9 \times 17.85 = 2387.21 \ kN$$

Using fig 12.16

for $d_b/d = 1$, $z_s/L = 7/17.85 = 0.4$

$$\& \left(\frac{S_o}{d}\right)\left(\frac{E_s}{\tau_a}\right) = 18$$

$$\frac{P_{max}}{P_{FS}} = 0.38$$

$$P_{max} = 900 \ kN$$

Using fig 12.17

$$z_s/L = 0.4, \quad \frac{S_o}{d} = \frac{0.056}{0.9} = 0.062$$

$$\frac{\rho}{S_o} = 0.15, \quad \rho = 0.15 \times 56 = 8.4 \ mm$$

b) Axial Load
of 50 kN

$\beta = \beta_o C_k C_v$

$K = \frac{E_p}{E_s} = 1740$

$L/d = \frac{17.85}{0.9} = 19.8$

from fig 5.11, 5.12 & 5.13

$\beta = 0.079$

Base load $= \beta \times P_{max} = 71.1$ kN

Max tensile force acts at depth of 0.5L or 8.9 m from top. Using fig 12.8 from Poulos. Part 3

At this level, axial force caused by applied load is 450 kN

→ Max tensile force = 900 − 450 = 450 kN

Pile movement by applied loading

$\rho = \frac{PI}{dE_s}$

Using fig 5.18 to 5.21 from Poulos

$\therefore I = 0.107$

$\rho = \frac{50000 \times 0.107}{0.9 \times 15.2 \times 10^6} = 0.39$ mm (downward)

Net movement caused by axial loading and swelling

→ $0.39 - 8.4 = 8.01$ mm (net upward movement)

→ Max Skin friction

$= \frac{450 \times 10^3}{\pi d l} = \cancel{152.15 \text{ kN/m}^2}$ 8.92 kN/m²

4. Pic showing Study results for Province

2)

Present Study

Stiffness of Pile $= \frac{AE}{L} = \frac{\frac{\pi}{4} \times 0.9^2 \times 21.5 \times 10^9}{17.85}$

$= 766258208.2 \ N/m$

Using PI & LL values from study & Suction value is directly estimated using Sucthen et al (1977) values by superimposing

$S_u = 383 \ kPa$

a) Pile movement by swelling

$\omega_s = \frac{S_u P L}{K} = \frac{383 \times 10^3 \times \pi \times 0.9 \times 17.85}{766258208.2}$

$= 25.2$ mm (upwards)

b) Pile movement by 50 kN loading

$I = 0.105$ (from previous Poulos)

$\rho = \frac{PI}{E_s d}$

$= \frac{50000 \times 0.105}{15.2 \times 10^6 \times 0.9} = 0.39$ mm (downward)

Net movement by axial loading & swelling

$0.39 - 25.2 = 24.8$ mm (net upward)

c) Max Skin friction

$= 0.5\left(\frac{2c'H + k\gamma H^2 \tan\phi}{L}\right) = 0.5(2 \times 5 \times 7 + 0.6 \times 19.5 \times 7^2 \tan 30)$

$= 11.23 \ kN/m^2$

d) Max Uplift Force

= Max Skin friction × Pile Surface Area

$= 566.89 \ kN$

5. Pic showing Poulos result for Nanning.

2 Nanning

PI = 43%

LL = 67.5%

Diameter of pile = 50 mm

Length of Pile = 0.65 m

Surface Swell, So (mm) = 41.2 mm

Active depth, ho = 0.58 m

Poisson's ratio, $v = 0.3$

Modulus of Elasticity, $E_p = 1.82$ GPa (for Pile)

Modulus of Elasticity of Soil, $E_s = 18.2$ MPa

Friction angle = 30

Horizontal earth pressure, $K_s = 0.6$

Unit weight of Soil = 18.7 kN/m$^3$

i) Poulo's

a) Zero Axial load

$$P_{FS} = \int_0^{0.65} \tau_a \pi d \, dz$$

$$\tau_a = K \gamma h \tan\phi$$

$$= 0.6 \times 18.7 \times 0.58 \times \tan\phi = 3.757 \text{ kN/m}^2$$

$$P_{FS} = 3.8 \times \pi \times 0.05 \times 0.65 = 0.388 \text{ kN, say } 0.4 \text{ kN}$$

Using fig 12.16

for $d_b/d = 1$ $\quad z_s/L = 0.58/0.65 = 0.89$

$$\& \left(\frac{S_o}{d}\right)\left(\frac{E_s}{\tau_a}\right) = 3990$$

$$\frac{P_{max}}{P_{FS}} = 0.5$$

$$P_{max} = 0.2 \text{ kN} \quad (\because 0.388 \times 0.5)$$

Using fig 12.17

$$z_s/L = 0.89, \quad \frac{S_o}{d} = 0.82$$

$$\frac{\rho}{S_o} = 0.3$$

$$\rho = 0.3 \times 41.2 = 12.36 \text{ mm}$$

b) Axial load of 1 kN

$\beta = \beta_0 C_k C_v$

$K = \frac{E_p}{E_s} = 1000$

$L/d = \frac{0.65}{0.05} = 13$

from fig 5.11, 5.12 & 5.13

$\beta = 0.078$

Base load $= \beta \times P_{max} = 0.2 \times 0.078 = 0.0156$ kN

Max tensile force acts at depth of 0.7L or 0.46 m from top. Using fig 12.8 from Poulos & Part 2

At this level, axial force caused by applied load is 0.06 kN

→ Max tensile force of $(0.2 - 0.06 = 0.14\text{ kN})$ ~~works~~ occurs at this point = 0.14 kN

Axial movement caused by loading

$\rho = \frac{PI}{E_s d}$

Using 5.18 to 5.21 figures from poulos

$\therefore I = 0.104$

$\rho = \frac{1000 \times 0.104}{1.82 \times 10^6 \times 0.05} = 1.1$ mm (downward)

→ Net movement caused by axial loading and swelling

$1.1 - 12.36 = 11.15$ mm (upward)

→ Max Skin friction

$= \frac{0.16}{\pi \times 0.05 \times 0.65} = 1.57$ kN/m²

6. Pic showing this study result for Nanning.

2) Present Study

Suction = 383 kPa, using PI & LL values from study & Suction value obtained by superimposing into table from Snethen et al (1977).

Stiffness of pile $= \frac{AE}{L} = \frac{\frac{\pi}{4} \times 0.05^2 \times 1.85 \times 10^9}{0.65} = 5588410.$ kN/m

Pile movement by swelling $= \frac{L \times P \times S}{K}$

$= \frac{0.65 \times \pi \times 0.05 \times 383 \times 10^3}{5588410.}$

$= 7$ mm (upward)

Pile movement by loading of 1kN

$\rho = \frac{P_u I}{E_s D}$

$I = 0.104$ (from previous Poulos)

$\rho = \frac{1000 \times 0.104}{18.2 \times 10^6 \times 0.05} = 1.1$ mm (downward)

Net movement caused by axial loading & swelling

$1.1 - 7 = 5.9$ mm (upward)

Max Skin friction

$= 0.5\left(2c'H + k\gamma H^2 \tan\phi\right)/L$

$= 0.5\left(2 \times 5 \times 0.58 + 0.6 \times 18.7 \times 0.58^2 \tan 30^\circ\right)/L$

$= 6.14$ kN/m$^2$

Max Axial force

= Max Skin friction × Area of pile surface

$= 3.99 \times \pi \times 0.05 \times 0.65$

$= 0.63$ kN

7. Pic showing Poulos result for Andhra.

Andhra

PI = 42.4 %

LL = 70.3 %

SG = 2.75

Diameter of Pile = 0.5 m = D

Length of Pile = 3.6 m = L

Surface swell, $s_0$ = 60 mm

Active depth, $h_0$ = 2 m

Modulus of elasticity of pile, $E_p$ = 26 GPa

Modulus of elasticity of Soil, $E_s$ = 15.2 MPa

Friction angle = 30°

Unit weight of soil = 17.6 kN/m³

1) Poulos

a) Zero axial load

$$P_{FS} = \int_0^{3.6} \tau_a \pi d \, dz$$

$$\tau_a = k \gamma h \tan\phi$$

$$= 0.6 \times 17.6 \times 2 \times \tan 30^\circ = 12.19$$

$$P_{FS} = \tau_a \times \pi \times 0.5 \times 3.6 = 68.95 \text{ kN}$$

Using fig 12.16

for $d_b/d = 1$ $\quad z_s/L = 2/3.6 = 0.55$

$$\alpha \left(\frac{s_0}{d}\right)\left(\frac{E_s}{\tau_a}\right) = 149$$

$$\frac{P_{max}}{P_{FS}} = 0.48$$

$$P_{max} = 0.48 \times 68.95 = 33 \text{ kN}$$

Using fig 12.17

$z_s/L = 0.55 \quad \frac{s_0}{d} = \frac{60}{500} = 0.12$

$$\frac{\rho}{s_0} = 0.25$$

$$\rho = 15 \text{ mm} = (0.25 \times 60)$$

b) Axial Load of 20 kN

$\beta = \beta_o C_k C_v$

$K = \frac{E_p}{E_s} = 1710$

$L/d = \frac{\cancel{3}3.6}{0.5} = 7.2$

from fig 5.11, 5.12 & 5.13

$\beta = 0.075$

Base load $= \beta \times P_{max} = 33 \times 0.075 = 2.475$ kN

Max tensile force acts at depth of 0.8L or 2.88m from top using fig 12.8 from Poulos, part 1

At this level axial force caused by applied load is 6.6 kN

→ Max tensile force of (33 − 6.6 = 26.4 kN) occurs at this point = 26.4 kN

Axial movement caused by loading

$\rho = \frac{PI}{E_s d}$

Using fig 5.18 to 5.21 from poulos

$I = 0.105$

$\rho = \frac{20000 \times 0.105}{15.2 \times 10^6 \times 0.5} = 0.3$ mm (downward)

→ Net movement caused by axial loading & swelling

$0.3 - 15 = 14.7$ mm (upward)

→ Max Skin friction

$= \frac{26.4}{\pi \times 0.5 \times 3.6} = 4.67$

8. Pic showing this study result for Andhra.

2) Study

PI & LL values given are superimposed in table of Snethen et al (1977) to obtain suction values

Suction = 383 kPa

Stiffness of pile $= \frac{AE}{L} = \frac{\frac{\pi}{4} \times 0.5^2 \times 26 \times 10^9}{3.6}$

$= 1418080001.7$ N/m

Pile movement by swelling $= \frac{L \times P \times S}{K}$

$= \frac{3.6 \times \pi \times 0.5 \times 383 \times 10^3}{1418080001.7}$

$= 15$ mm

Pile movement by 20 kN Loading

$I = 0.105$ (obtained from fig 5.18 to 5.21 from Poulos)

$\rho = \frac{20000 \times 0.105}{15.2 \times 10^6 \times 0.5} = 0.3$ mm (downward)

→ Net movement caused by axial loading & swelling

$0.3 - 15 = 14.7$ mm (upward)

→ Max skin friction

$= 0.5\,(2c'H + K\gamma H^2 \tan\phi)/L$

$= 0.5\,(2 \times 5 \times 2 + 0.6 \times 17.6 \times 2^2 \tan 30^\circ)/3.6$

$= 6.16$ kN/m$^2$

Max Axial force

$=$ Max Skin friction $\times \pi d \times L$

$= 34.86$ kN

# Appendix E - Results from Silva 2022 using Excel Spreadsheet

1. Province Result from excel spreadsheet

| | A | B | C | D | E | F | G | H | I |
|---|---|---|---|---|---|---|---|---|---|
| 1 | | | | | | | | alpha | |
| 2 | Radius of pile | ro | 0.45 | | c3 | 374.4724204 | -374.4724204 | -0.008571428571 | |
| 3 | Length of pile | L | 16.5 | | c4 | 0.04727272698 | 0.04727272698 | 0.000001082041776 | |
| 4 | Shear Modulus | Gs | 5.85 | | c5 | 0.00000480676249 | 0.00000480676249 | 0.0000000001100236 | |
| 5 | Poisson's Ratio | v | 0.3 | | c6 | 0.01272727328 | -0.01272727328 | -0.0000002913189539 | |
| 6 | Modulus of Elasticity | E | 2150000000 | | | | | | |
| 7 | Area of Pile | A | 0.63585 | 16850025000 | | | | | |
| 8 | | | | | H | z | L | | |
| 9 | inundation pressure | σ'i | 44.37 | cos | 1.000000 | 1 | 1.000000071 | | |
| 10 | unit weight | 19.5 | | sin | 0.000160 | 0 | 0.000377674208 | | |
| 11 | | | | | | | | | |
| 12 | | | | | | | | | |
| 13 | Surface Area | 46.629 | | | | Depth | Axial Force Induced (kN) | Skin Friction (kPa) | Net Movement (mm) |
| 14 | | λp | 4529914530 | | | 0 | 0 | 0 | 12.7 |
| 15 | | rm | 28.875 | | | 1 | 208.72 | 4.472727273 | 12.7 |
| 16 | | | | | | 2 | 375.82 | 8.054545455 | 12.7 |
| 17 | | ζ | 4.161483865 | | | 3 | 501.3 | 10.74545455 | 12.7 |
| 18 | | | | | | 4 | 585.17 | 12.54909091 | 12.7 |
| 19 | | α | 0.000022889 | | | 5 | 627.4 | 13.45454545 | 12.7 |
| 20 | | | | so/H | | 6 | 628.05 | 13.46787879 | 12.7 |
| 21 | | So | 0.06 | 0.008571428571 | | 7 | 587 | 12.58969697 | 12.7 |
| 22 | Check depth | z | 0 | So(H-z) / H | | 8 | 525.5 | 11.26484848 | 12.7 |
| 23 | Active Depth Layer | H | 7 | 0.06 | | 9 | 463.4 | 9.939393939 | 12.7 |
| 24 | | | | | | 10 | 401.67 | 8.612121212 | 12.7 |
| 25 | | P1 (z) kN | 0 <z <H | 0 | | 11 | 339.8 | 7.288484848 | 12.7 |
| 26 | | P2 (z) kN | H <z <L | 1019.64566 | | 12 | 278 | 5.963636364 | 12.7 |
| 27 | shaft friction | | 0 | 21.86719981 | | 13 | 216.2 | 4.636363636 | 12.7 |
| 28 | displacement | W1 (z) mm | 0 <z <H | -12.72727302 | | 14 | 154.49 | 3.312727273 | 12.7 |
| 29 | | W2 (z) mm | H <z <L | -12.72727328 | | 15 | 92.69 | 1.987878788 | 12.7 |
| 30 | | | | | | 16 | 30.8 | 0.6606060606 | 12.7 |
| 31 | strain | w'1 (z) | 0 <z <H | 0 | | | | | |
| 32 | | w'2 (z) | H <z <L | 0.0000000001100 | | | | | |
| 33 | | | | | | | | | |
| 34 | | | | | | | | | |
| 35 | | | | | | | | | |
| 36 | | | | | | | | | |
| 37 | | | | | | | | | |
| 38 | | | | | | | | | |

Changing check depth only

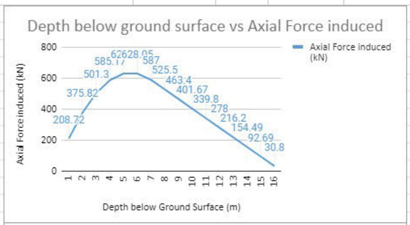


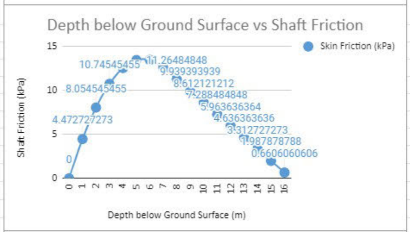


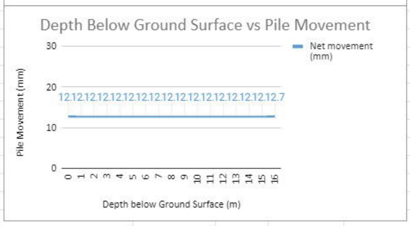

## 2. Colorado Result from excel spreadsheet

| | A | B | C | D | E | F | G | H | I |
|---|---|---|---|---|---|---|---|---|---|
| 1 | | | | | | | | alpha | |
| 2 | Radius of pile | ro | 0.25 | | c3 | 225.8851454 | -225.8851454 | -0.008571428571 | |
| 3 | Length of pile | L | 19.3 | | c4 | 0.04911916968 | 0.04911916968 | 0.000001863874022 | |
| 4 | Shear Modulus | Gs | 5.85 | | c5 | 0.000007968651545 | 0.00000796865154 | 0.00000000030237812 | |
| 5 | Poisson's Ratio | v | 0.3 | | c6 | 0.01088083103 | -0.01088083103 | -0.0000004128835731 | |
| 6 | Modulus of Elasticity | E | 3250000000 | | | | | | |
| 7 | Area of Pile | A | 0.19625 | 5200625000 | | | | | |
| 8 | | | | | H | z | L | | |
| 9 | inundation pressure | σ'i | 44.37 | cos | 1.000000 | 1.000000026 | 1.000000268 | | |
| 10 | unit weight | 19.5 | | sin | 0.000265 | 0.0002276757588 | 0.0007323570833 | | |
| 11 | | | | | | | | | |
| 12 | | | | | | | | | |
| 13 | Surface Area | 30.301 | | | | Depth | Axial Force Induced (kN) | Skin Friction (kPa) | Net Movement (mm) |
| 14 | | λp | 4529914530 | | | 0 | 0 | 0 | 10.8 |
| 15 | | rm | 33.775 | | | 1 | 50.3 | 1.658031088 | 10.8 |
| 16 | | | | | | 2 | 91.09 | 3.005181347 | 10.8 |
| 17 | | ζ | 4.906015245 | | | 3 | 122.19 | 4.031088083 | 10.8 |
| 18 | | | | | | 4 | 143.67 | 4.740932642 | 10.8 |
| 19 | | α | 0.000037945 | | | 5 | 155.5 | 5.129533679 | 10.8 |
| 20 | | | | so/H | | 6 | 157.73 | 5.207253886 | 10.8 |
| 21 | | So | 0.06 | 0.008571428571 | | 7 | 150.3 | 4.958549223 | 10.8 |
| 22 | Check depth | z | 6 | So(H-z) / H | | 8 | 138.1 | 4.398963731 | 10.8 |
| 23 | Active Depth Layer | H | 7 | 0.008571428571 | | 9 | 125.88 | 4.154404145 | 10.8 |
| 24 | | | | | | 10 | 113.66 | 3.750777202 | 10.8 |
| 25 | | P1 (z) kN | 0 <z <H | 157.7377438 | | 11 | 101.44 | 3.347150259 | 10.8 |
| 26 | | P2 (z) kN | H <z <L | 162.5516885 | | 12 | 89.22 | 2.943005181 | 10.8 |
| 27 | shaft friction | | 5.205694326 | 5.364565146 | | 13 | 76.9 | 2.538860104 | 10.8 |
| 28 | displacement | W1 (z) mm | 0 <z <H | -10.88082949 | | 14 | 64.7 | 2.129533679 | 10.8 |
| 29 | | W2 (z) mm | H <z <L | -10.88083131 | | 15 | 52.5 | 1.730569948 | 10.8 |
| 30 | | | | | | 16 | 40.3 | 1.32642487 | 10.8 |
| 31 | strain | w'1 (z) | 0 <z <H | 0.0000000002022 | | 17 | 28.11 | 0.9274611399 | 10.8 |
| 32 | | w'2 (z) | H <z <L | 0.0000000002083 | | 18 | 15.8 | 0.5233160622 | 10.8 |
| 33 | | | | | | 19 | 3.6 | 0.1191709845 | 10.8 |

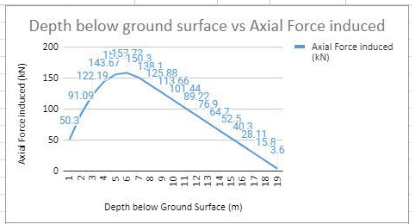


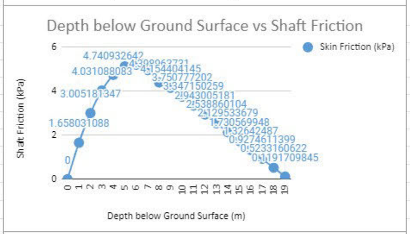


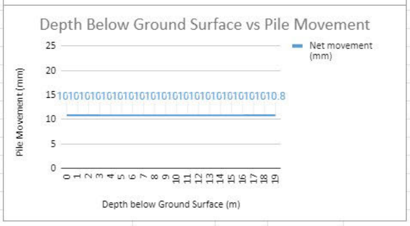

## 3. Nanning Result from excel spreadsheet

| | A | B | C | D | E | F | G | H | I |
|---|---|---|---|---|---|---|---|---|---|
| 1 | | | | | | | | alpha | |
| 2 | Radius of pile | ro | 0.05 | | c3 | 77.92259777 | -77.92259777 | -0.07068965517 | |
| 3 | Length of pile | L | 0.65 | | c4 | 0.02270769165 | 0.02270769165 | 0.00002059991502 | |
| 4 | Shear Modulus | Gs | 5.85 | | c5 | 0.00001078634496 | 0.00001078634496 | 0.000000009785133 | |
| 5 | Poisson's Ratio | v | 0.3 | | c6 | 0.01829231024 | -0.01829231024 | -0.00001659437878 | |
| 6 | Modulus of Elasticity | E | 1820000000 | | | | | | |
| 7 | Area of Pile | A | 0.00785 | 14287000 | | | | | |
| 8 | | | | | H | z | L | | |
| 9 | inundation pressure | σ'i | 44.37 | cos | 1.000000 | 1.000000148 | 1.000000174 | | |
| 10 | unit weight | 18.7 | | sin | 0.000526 | 0.0005443067404 | 0.0005896656405 | | |
| 13 | Surface Area | 0.2041 | | | | Depth | Axial Force Induced (kN) | Skin Friction (kPa) | Net Movement (mm) |
| 14 | | λp | 311111111.1 | | | 0.1 | 0.23 | 1.107692308 | 9.14 |
| 15 | | rm | 1.1375 | | | 0.2 | 0.37 | 1.8 | 9.14 |
| 16 | | | | | | 0.3 | 0.42 | 2.092307692 | 9.14 |
| 17 | | ζ | 3.124565145 | | | 0.4 | 0.4 | 1.969230769 | 9.14 |
| 18 | | | | | | 0.5 | 0.3 | 1.446153846 | 9.14 |
| 19 | | α | 0.00090717 | | | 0.6 | 0.1 | 0.5230769231 | 9.14 |
| 20 | | | | so/H | | | | | |
| 21 | | So | 0.041 | 0.07068965517 | | | | | |
| 22 | Check depth | z | 0.6 | So(H-z) / H | | | | | |
| 23 | Active Depth Layer | H | 0.58 | -0.001413793103 | | | | | |
| 25 | | P1 (z) kN | 0 <z <H | 0.1058762997 | | | | | |
| 26 | | P2 (z) kN | H <z <L | 0.1075386085 | | | | | |
| 27 | shaft friction | | 0.518747181 | 0.5268917615 | | | | | |
| 28 | displacement (m) | W1 (z) mm | 0 <z <H | -9.14615354 | | | | | |
| 29 | | W2 (z) mm | H <z <L | -9.14615354 | | | | | |
| 31 | strain | w'1 (z) | 0 <z <H | 0.000000000741 | | | | | |
| 32 | | w'2 (z) | H <z <L | 0.0000000007527 | | | | | |

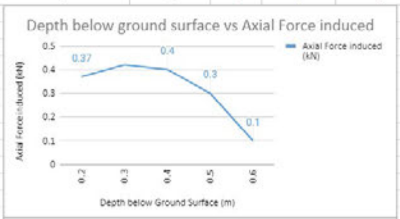


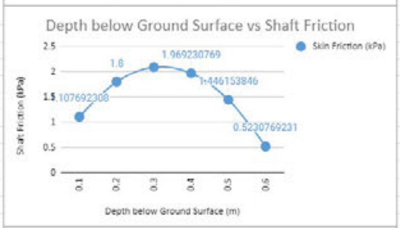


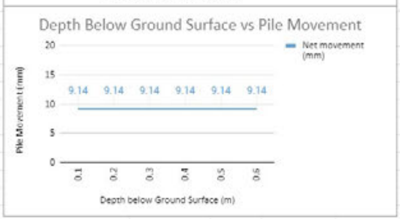

## 4. Andhra Result from excel spreadsheet

F34

| | A | B | C | D | E | F | G | H | I |
|---|---|---|---|---|---|---|---|---|---|
| 1 | | | | | | | | alpha | |
| 2 | Radius of pile | ro | 0.5 | | c3 | 1136.314603 | -1136.314603 | -0.03 | |
| 3 | Length of pile | L | 3.6 | | c4 | 0.04333333433 | 0.04333333433 | 0.000001144049392 | |
| 4 | Shear Modulus | Gs | 5.85 | | c5 | 0.000001584068286 | 0.00000158406828 | 0 | |
| 5 | Poisson's Ratio | v | 0.3 | | c6 | 0.0166666657 | -0.0166666657 | -0.000000440018961 | |
| 6 | Modulus of Elasticity | E | 2600000000 | | | | | | |
| 7 | Area of Pile | A | 0.785 | 20802500000 | | | | | |
| 8 | | | | | H | z | L | | |
| 9 | inundation pressure | σ'i | 44.37 | cos | 1.000000 | 1.000000004 | 1.000000005 | | |
| 10 | unit weight | 19.5 | | sin | 0.000052 | 0.00009240398733 | 0.00009504410126 | | |
| 11 | | | | | | | | | |
| 12 | | | | | | | | | |
| 13 | Surface Area | 11.304 | | | | Depth | Axial Force Induced (kN) | Skin Friction (kPa) | Net Movement (mm) |
| 14 | | λp | 4529914530 | | | 0 | 0 | 0 | 16.67 |
| 15 | | rm | 6.3 | | | 0.5 | 26 | 2.297222222 | 16.67 |
| 16 | | | | | | 1 | 41.08 | 3.633333333 | 16.67 |
| 17 | | ζ | 2.53369681 | | | 1.5 | 45.31 | 4.008333333 | 16.67 |
| 18 | | | | | | 2 | 38.66 | 3.420555556 | 16.67 |
| 19 | | α | 0.00002640 | | | 2.5 | 26.58 | 1.869444444 | 16.67 |
| 20 | | | | so/H | | 3 | 14.5 | 1.283333333 | 16.67 |
| 21 | | So | 0.06 | 0.03 | | 3.5 | 2.41 | 0.2138888889 | 16.67 |
| 22 | Check depth | z | 3.5 | So(H-z) / H | | | | | |
| 23 | Active Depth Layer | H | 2 | -0.045 | | | | | |
| 24 | | | | | | | | | |
| 25 | | P1 (z) kN | 0 <z <H | -46.52006851 | | | | | |
| 26 | | P2 (z) kN | H <z <L | 2.416628523 | | | | | |
| 27 | shaft friction | | -4.11536345 | 0.213785255 | | | | | |
| 28 | displacement | W1 (z) mm | 0 <z <H | -16.66666563 | | | | | |
| 29 | | W2 (z) mm | H <z <L | -16.66666562 | | | | | |
| 30 | | | | | | | | | |
| 31 | strain | w'1 (z) | 0 <z <H | 0 | | | | | |
| 32 | | w'2 (z) | H <z <L | 0 | | | | | |
| 33 | | | | | | | | | |
| 34 | | | | | | | | | |
| 35 | | | | | | | | | |
| 36 | | | | | | | | | |
| 37 | | | | | | | | | |
| 38 | | | | | | | | | |

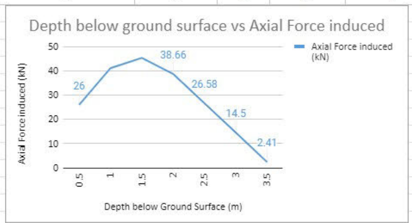


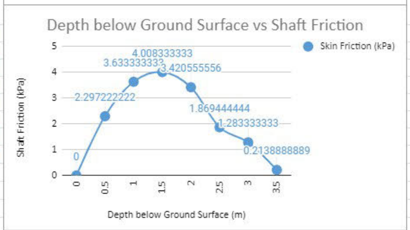


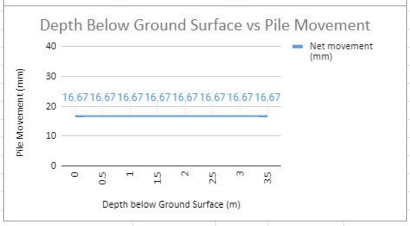

# Appendix F – Numerical Results from RSPile

1. Pic showing RS Pile result for Province.

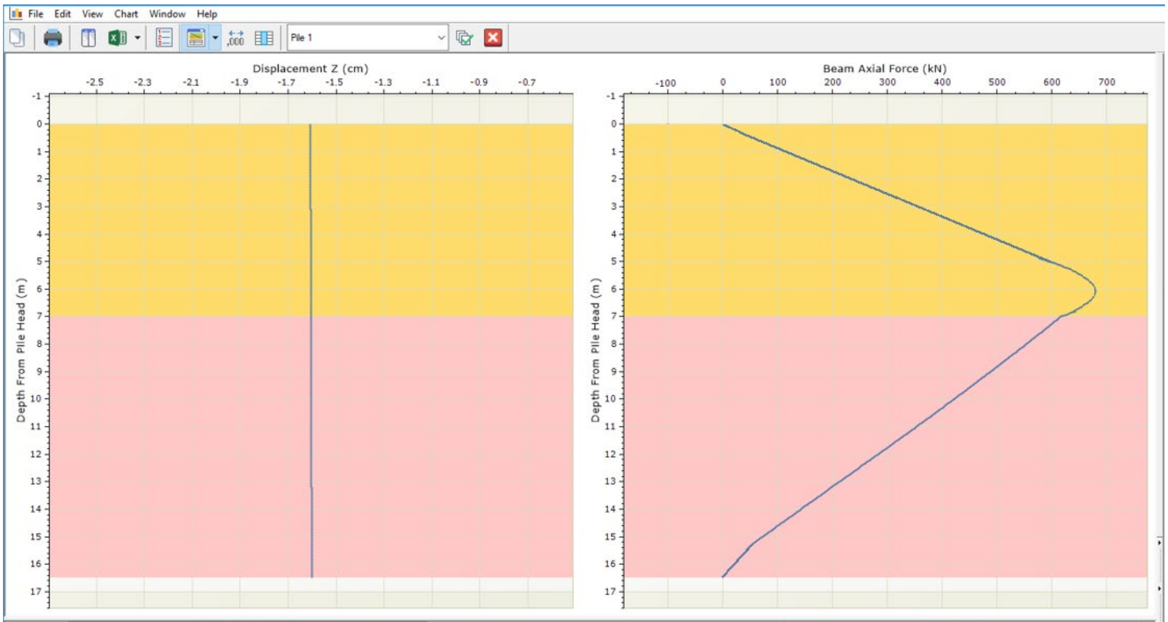


| | Depth From Pile Head (m) | Displacement Z (cm) | Beam Axial Force (kN) |
|---|---|---|---|
| 1 | 0.000 | -1.61 | -0.653 |
| 2 | 0.041 | -1.61 | 1.319 |
| 3 | 0.082 | -1.61 | 4.092 |
| 4 | 0.124 | -1.61 | 7.488 |
| 5 | 0.165 | -1.61 | 11.018 |
| 6 | 0.206 | -1.61 | 14.900 |
| 7 | 0.247 | -1.61 | 18.879 |
| 8 | 0.288 | -1.61 | 23.117 |
| 9 | 0.329 | -1.61 | 27.430 |
| 10 | 0.371 | -1.61 | 31.951 |
| 11 | 0.412 | -1.61 | 36.536 |
| 12 | 0.453 | -1.61 | 41.295 |
| 13 | 0.494 | -1.61 | 46.109 |
| 14 | 0.535 | -1.61 | 51.076 |
| 15 | 0.576 | -1.61 | 56.091 |
| 16 | 0.618 | -1.61 | 61.242 |
| 17 | 0.659 | -1.61 | 66.437 |
| 18 | 0.700 | -1.61 | 71.754 |
| 19 | 0.741 | -1.61 | 77.111 |
| 20 | 0.782 | -1.61 | 82.581 |
| 21 | 0.824 | -1.61 | 88.086 |
| 22 | 0.865 | -1.61 | 93.696 |
| 23 | 0.906 | -1.61 | 99.340 |
| 24 | 0.947 | -1.61 | 105.080 |

Results

7 mm swell 56 skin - Plan/3D View | 7 mm swell 56 skin - Results

Ready MAX DATATIPS SNAP GRID ORTHO OSNAP

2. RS Pile result for Province

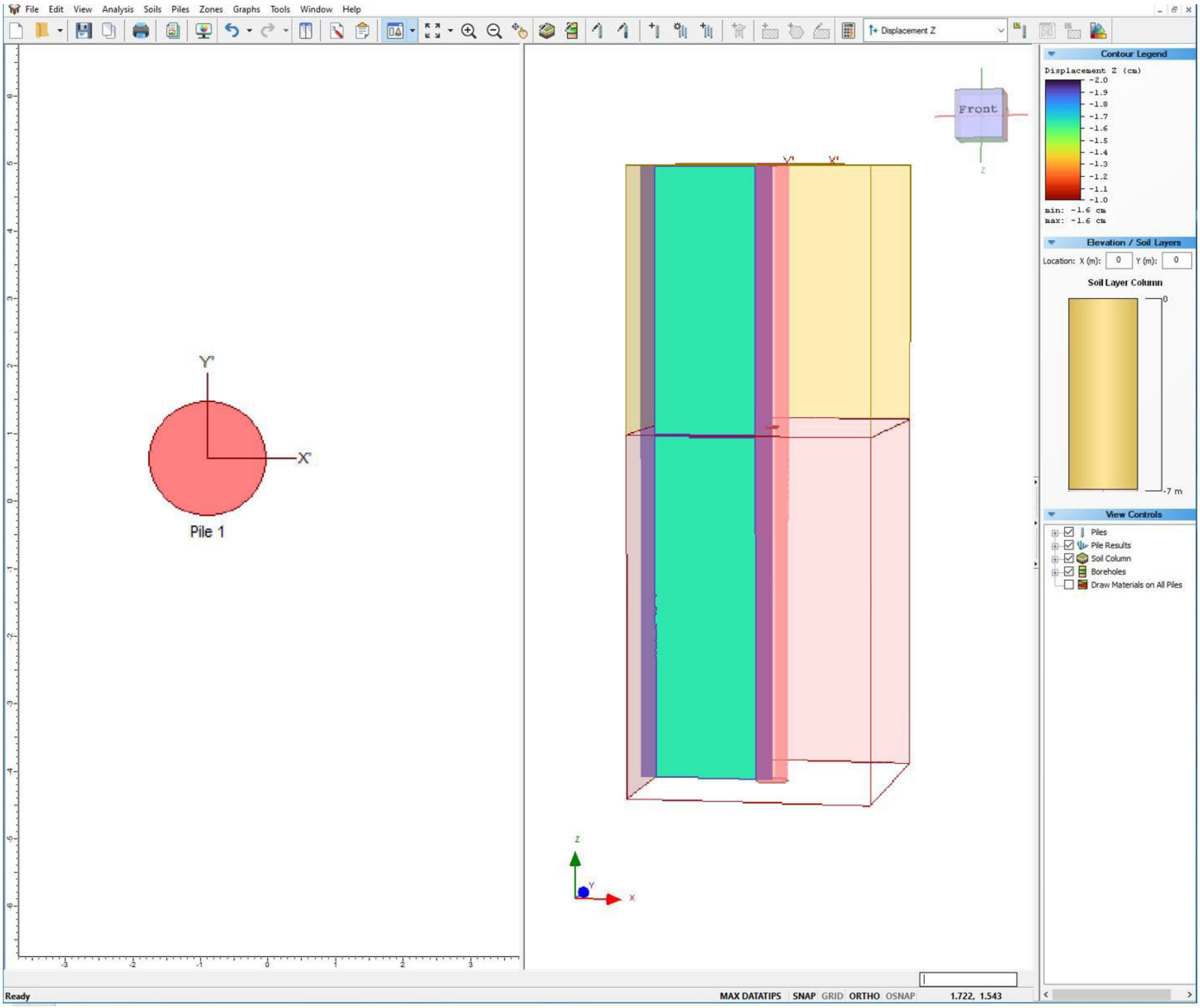

3. RS Pile for Nanning

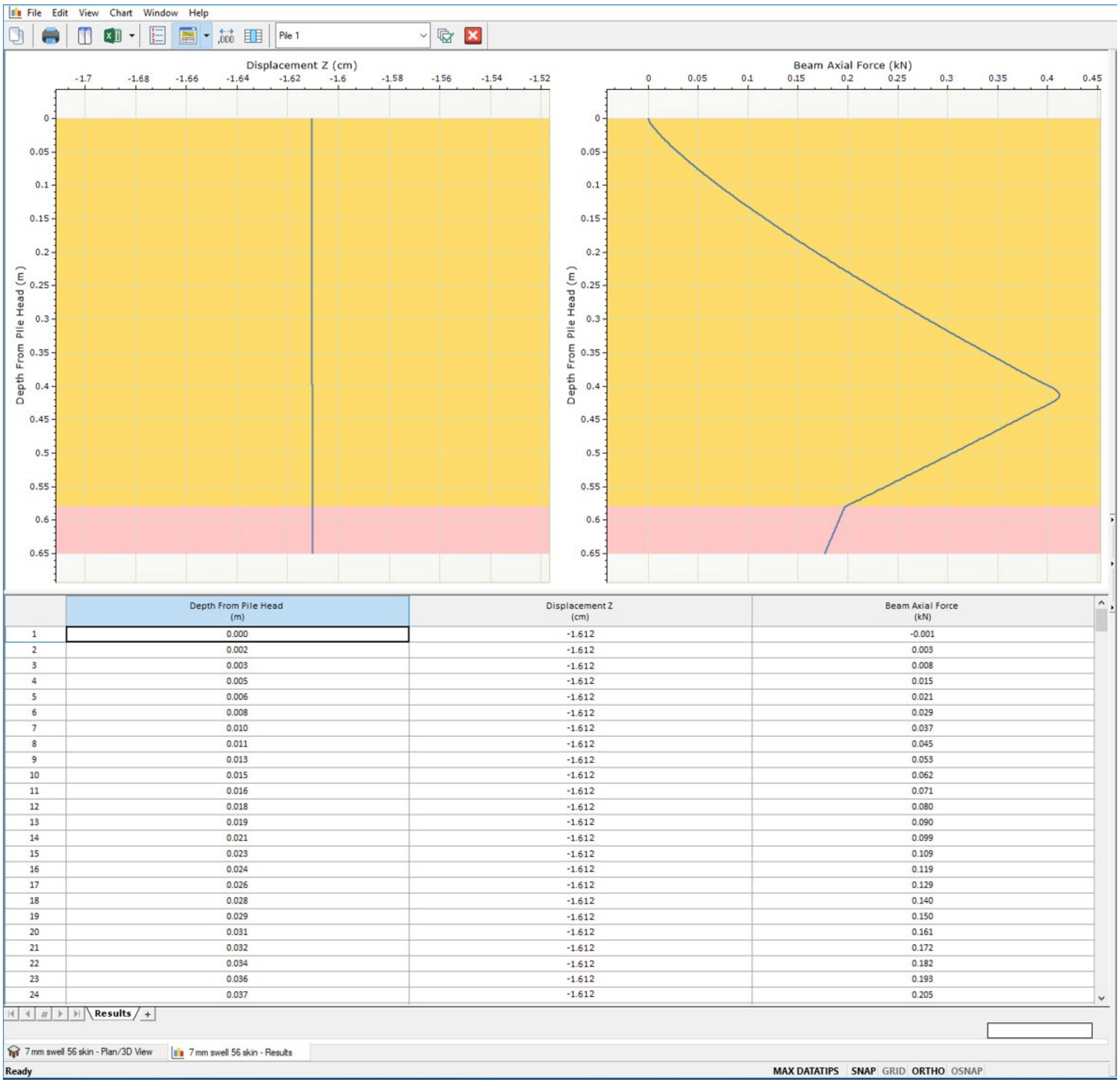


| | Depth From Pile Head (m) | Displacement Z (cm) | Beam Axial Force (kN) |
|---|---|---|---|
| 1 | 0.000 | -1.612 | -0.001 |
| 2 | 0.002 | -1.612 | 0.003 |
| 3 | 0.003 | -1.612 | 0.008 |
| 4 | 0.005 | -1.612 | 0.015 |
| 5 | 0.006 | -1.612 | 0.021 |
| 6 | 0.008 | -1.612 | 0.029 |
| 7 | 0.010 | -1.612 | 0.037 |
| 8 | 0.011 | -1.612 | 0.045 |
| 9 | 0.013 | -1.612 | 0.053 |
| 10 | 0.015 | -1.612 | 0.062 |
| 11 | 0.016 | -1.612 | 0.071 |
| 12 | 0.018 | -1.612 | 0.080 |
| 13 | 0.019 | -1.612 | 0.090 |
| 14 | 0.021 | -1.612 | 0.099 |
| 15 | 0.023 | -1.612 | 0.109 |
| 16 | 0.024 | -1.612 | 0.119 |
| 17 | 0.026 | -1.612 | 0.129 |
| 18 | 0.028 | -1.612 | 0.140 |
| 19 | 0.029 | -1.612 | 0.150 |
| 20 | 0.031 | -1.612 | 0.161 |
| 21 | 0.032 | -1.612 | 0.172 |
| 22 | 0.034 | -1.612 | 0.182 |
| 23 | 0.036 | -1.612 | 0.193 |
| 24 | 0.037 | -1.612 | 0.205 |

4. RS Pile for Nanning

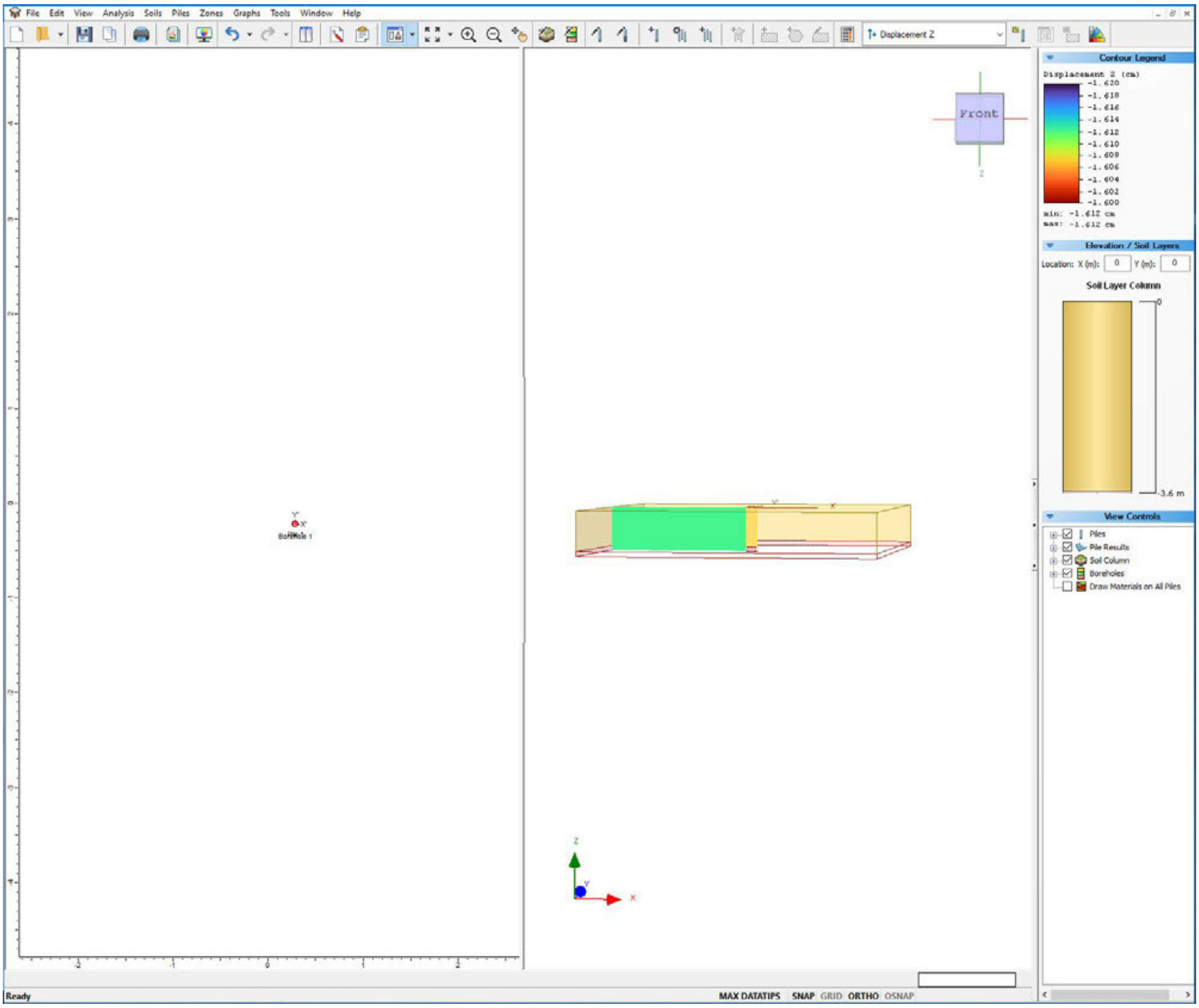

5. RS Pile for Colorado

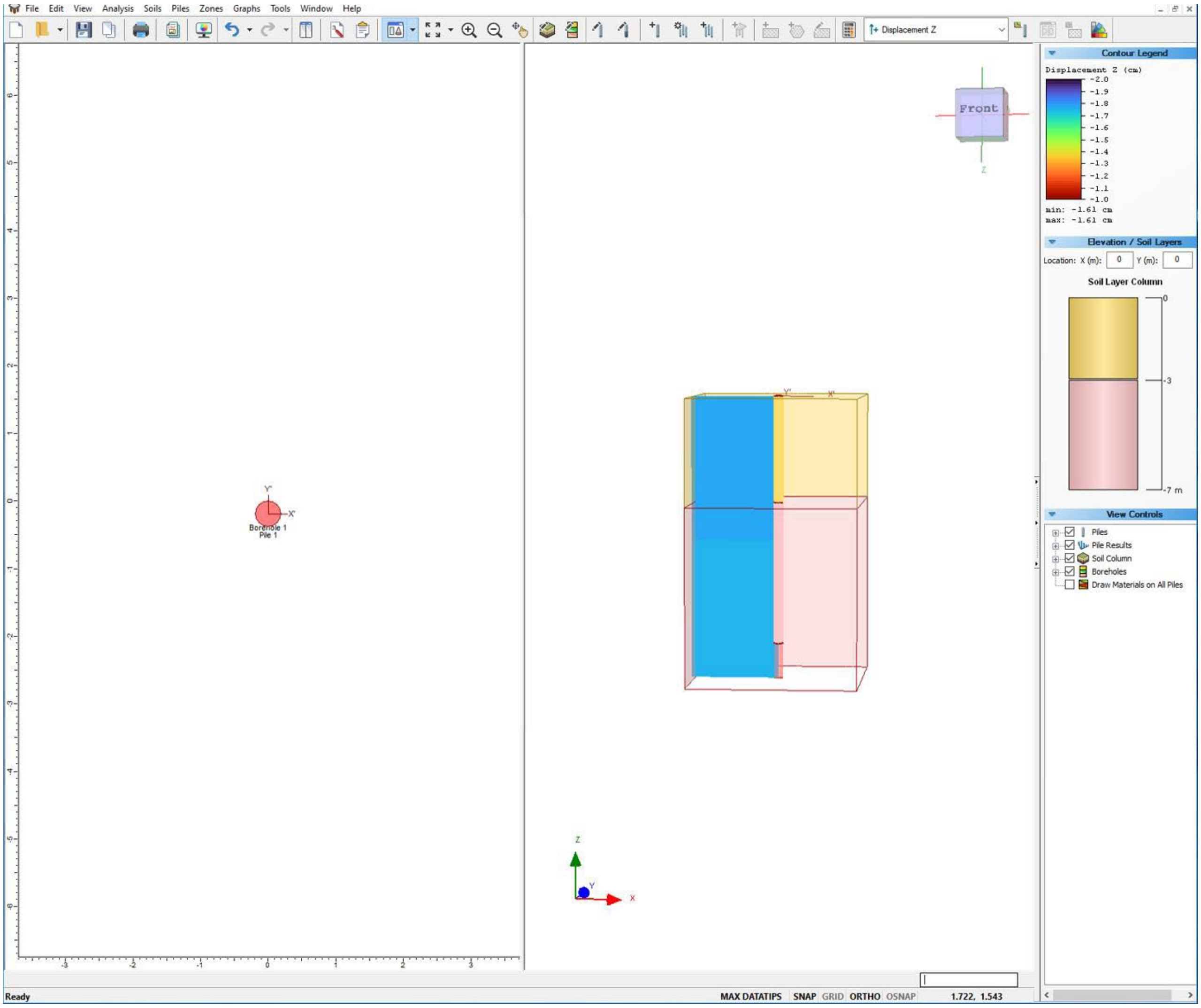

## 6. RS Pile for Colorado

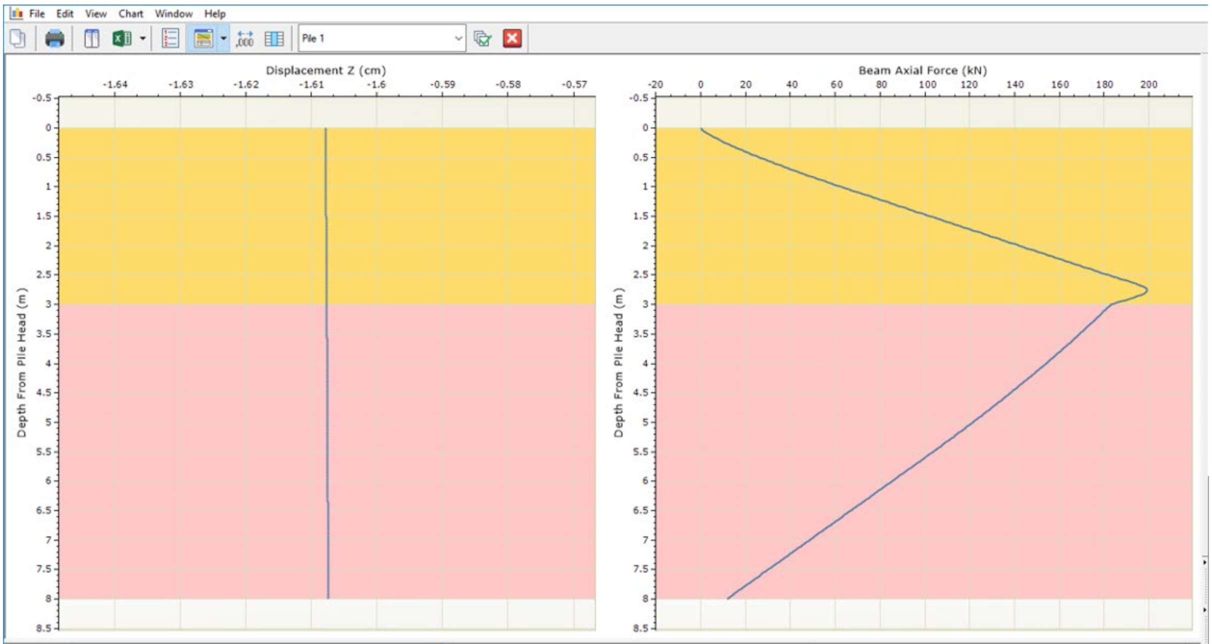


| | Depth From Pile Head (m) | Displacement Z (cm) | Beam Axial Force (kN) |
|---|---|---|---|
| 1 | 0.000 | -1.608 | -0.073 |
| 2 | 0.020 | -1.608 | 0.149 |
| 3 | 0.040 | -1.608 | 0.461 |
| 4 | 0.060 | -1.608 | 0.844 |
| 5 | 0.080 | -1.608 | 1.241 |
| 6 | 0.100 | -1.608 | 1.678 |
| 7 | 0.120 | -1.608 | 2.127 |
| 8 | 0.140 | -1.608 | 2.604 |
| 9 | 0.160 | -1.608 | 3.090 |
| 10 | 0.180 | -1.608 | 3.599 |
| 11 | 0.200 | -1.608 | 4.115 |
| 12 | 0.220 | -1.608 | 4.651 |
| 13 | 0.240 | -1.608 | 5.194 |
| 14 | 0.260 | -1.608 | 5.753 |
| 15 | 0.280 | -1.608 | 6.318 |
| 16 | 0.300 | -1.608 | 6.898 |
| 17 | 0.320 | -1.608 | 7.483 |
| 18 | 0.340 | -1.608 | 8.082 |
| 19 | 0.360 | -1.608 | 8.685 |
| 20 | 0.380 | -1.608 | 9.301 |
| 21 | 0.400 | -1.608 | 9.922 |
| 22 | 0.420 | -1.608 | 10.553 |
| 23 | 0.440 | -1.608 | 11.189 |
| 24 | 0.460 | -1.608 | 11.836 |

Results

7. RS Pile for Andhra

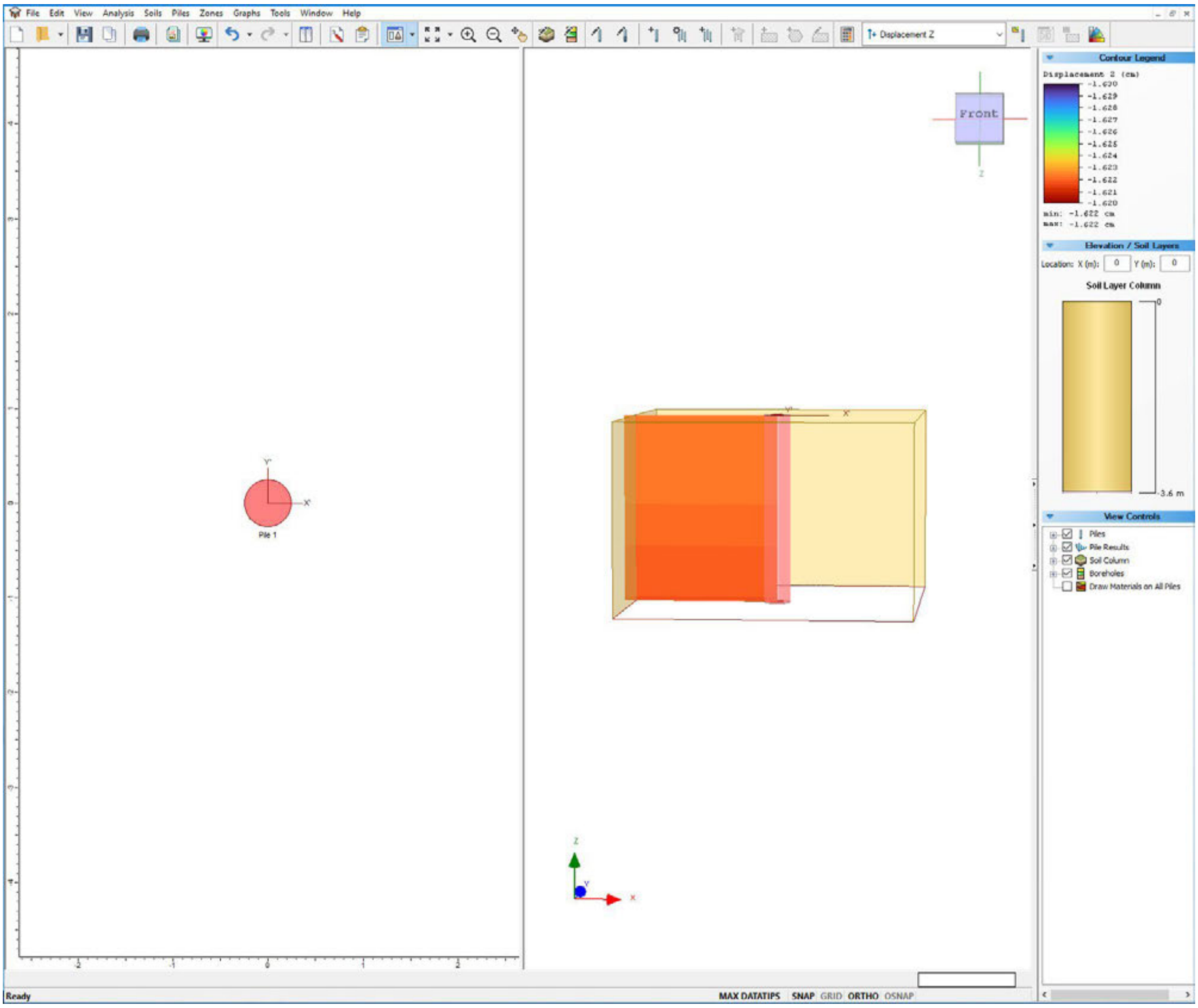

## 8. RS Pile for Andhra

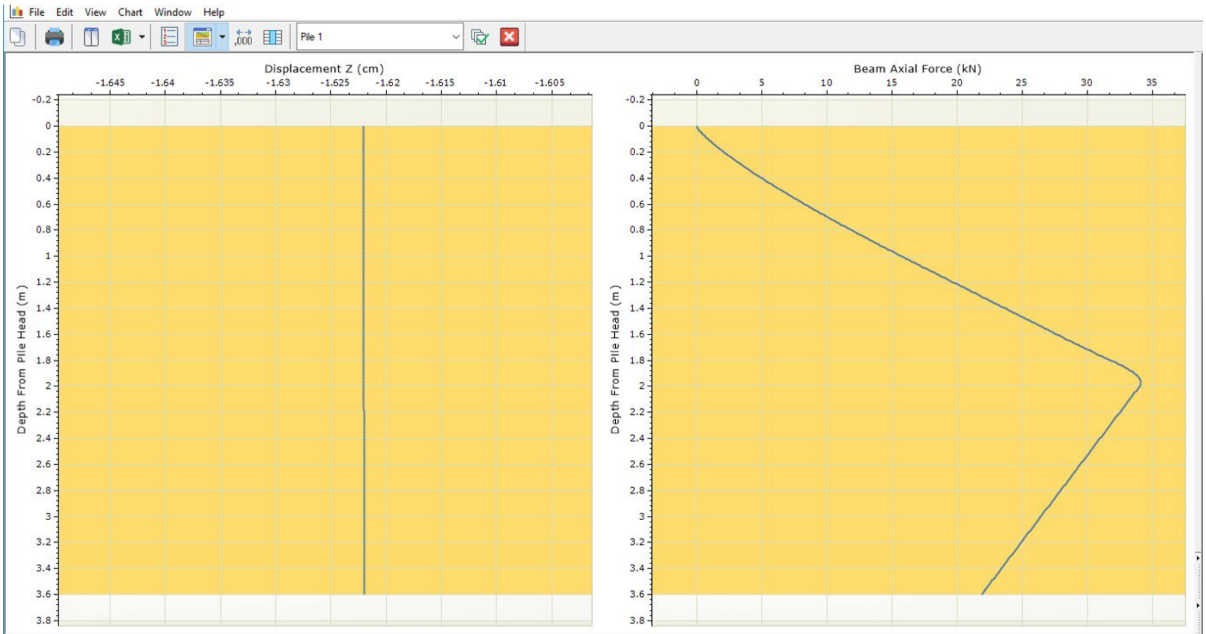


| | Depth From Pile Head (m) | Displacement Z (cm) | Beam Axial Force (kN) |
|---|---|---|---|
| 1 | 0.000 | -1.622 | -0.054 |
| 2 | 0.009 | -1.622 | 0.110 |
| 3 | 0.018 | -1.622 | 0.340 |
| 4 | 0.027 | -1.622 | 0.622 |
| 5 | 0.036 | -1.622 | 0.915 |
| 6 | 0.045 | -1.622 | 1.237 |
| 7 | 0.054 | -1.622 | 1.568 |
| 8 | 0.063 | -1.622 | 1.919 |
| 9 | 0.072 | -1.622 | 2.278 |
| 10 | 0.081 | -1.622 | 2.653 |
| 11 | 0.090 | -1.622 | 3.034 |
| 12 | 0.099 | -1.622 | 3.429 |
| 13 | 0.108 | -1.622 | 3.828 |
| 14 | 0.117 | -1.622 | 4.241 |
| 15 | 0.126 | -1.622 | 4.657 |
| 16 | 0.135 | -1.622 | 5.085 |
| 17 | 0.144 | -1.622 | 5.516 |
| 18 | 0.153 | -1.622 | 5.958 |
| 19 | 0.162 | -1.622 | 6.402 |
| 20 | 0.171 | -1.622 | 6.857 |
| 21 | 0.180 | -1.622 | 7.314 |
| 22 | 0.189 | -1.622 | 7.779 |
| 23 | 0.198 | -1.622 | 8.248 |
| 24 | 0.207 | -1.622 | 8.725 |

Results